AD-A090 326 ROCKWELL INTERNATIONAL ANAHEIM CA ELECTRONICS RESEAR--ETC F/G 20/5
ROOM TEMPERATURE, CW, SINGLE MODE LASER.(U)
OCT 80 P D DAPKUS, J J COLEMAN, R D DUPUIS N00173-79-C-0025
UNCLASSIFIED C80-636/501 NL

1 OF 1
AD A 090326

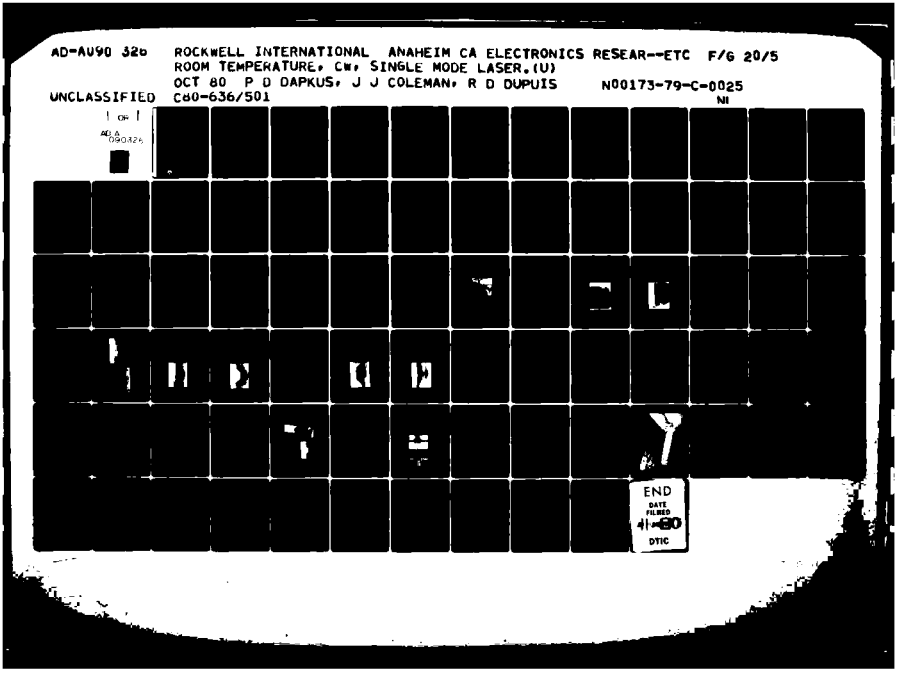

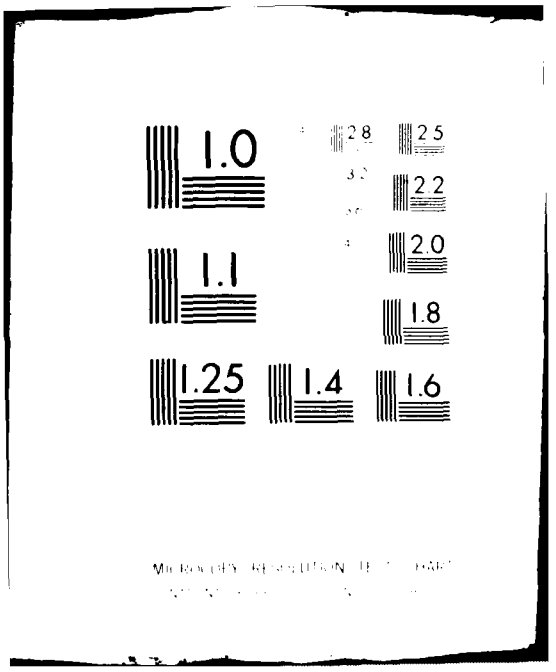
1.0
2.8
2.5
2.2
2.0
1.1
1.8
1.25
1.4
1.6

C80-636/501

FINAL TECHNICAL REPORT

ROOM TEMPERATURE, CW, SINGLE MODE LASER

CONTRACT NO. N00173-79-C-0025

OCTOBER 1, 1980

PREPARED FOR:

DR. T. G. GIALLORENZI
NAVAL RESEARCH LABORATORY
WASHINGTON, D C 20375

APPROVED FOR PUBLIC RELEASE; DISTRIBUTION UNLIMITED

PREPARED BY:

P. D. DAPKUS, PROGRAM MANAGER
ROCKWELL INTERNATIONAL
ELECTRONICS RESEARCH CENTER
3370 MIRALOMA AVENUE
ANAHEIM, CALIFORNIA 92803

A

Rockwell International

C80-636/501

FINAL TECHNICAL REPORT

ROOM TEMPERATURE, CW, SINGLE MODE LASER

CONTRACT NO. N00173-79-C-0025

October 1, 1980

Prepared by:

P. D. Dapkus, Program Manager

Rockwell International
Electronics Research Center
3370 Miraloma Avenue
Anaheim, California 92803

A

ABSTRACT

This report describes results obtained in the study of single mode cw room temperature diode lasers. Three device designs are analyzed and studied. Detailed calculations on the modal properties of channel guide lasers have been performed. Experimental studies of the transverse junction stripe laser, channel guide laser, inverted channel guide laser and self-aligned structure laser have been made. This last device has operated on a fundamental mode with cw room temperature thresholds much lower than 100 mA. Device packaging is described including a Si submount and an optical fiber pigtail in a hermetically sealed package. Details of the developments undertaken and the results obtained are discussed.

TABLE OF CONTENTS

LIST OF FIGURES

1.0 INTRODUCTION

This report constitutes the final report for Contract No. N00173-79-C-0025 entitled "Single Mode CW Room Temperature Diode Lasers," performed by the Electronics Research Center of Rockwell International for the Naval Research Laboratory. Dr. Thomas Giallorenzi served as the contract monitor and Dr. J.J. Coleman and Dr. R.D. Dupuis served as principal investigators during the course of the program.

The program was an ambitious one whose ultimate goal was to produce single mode CW lasers to be used for a variety of Navy signal processing requirements. The specific goals of the device development best expressed in the desired device characteristics:

1. Threshold current I_{th} = 25 ma
2. Voltage V = 2.0 volts
3. Single longitudinal and transverse modes at powers up to 4 mw/facet and at currents up to two times threshold.
4. Spectral bandwidth below 10^{-1} 19° high currents.
5. Beam Ellipticity < 3:1
6. External differential quantum efficiency. > 20%
7. Lifetime (20°C) 10^4 hrs.
8. CW operation to 70°C.
9. Non-active heat sinking to 70°C.

These characteristics place stringent requirements on the design of the device and at the time of the solicitation had not been achieved in total in any device design.

In addition to this device design and development there was to be activity directed towards the packaging of these devices. The goal of this work was to produce a hermetically sealed device structure containing a fiber pigtail that satisfied Mil Spec E5400. The combination of these device and packaging requirements resulted in a most ambitious program.

Rockwell/ERC's approach to the problems embodied in these program goals was based on a combination of previously developed device designs and packaging concepts as well as new concepts designed to improve device performance and remove as much as possible the "art" associated with packaging and bonding the devices. In general the program was successful although not all goals of the program were met. The purpose of this report is to describe the progress achieved on the program toward these goals and to discuss the development necessary to achieve all of them.

1.1 Device Designs

Three device designs were investigated during the course of this program to achieve the goals outlined above. These designs are illustrated schematically in Figs. 1.1.1 and 1.1.2. The channel guide structure is a modification of a device structure previously demonstrated by Rockwell[1] to operate in a single longitudinal and transverse mode. The original device structure had no substrate confinement and lased at 200 mA CW for a 380 μm long device. In addition the mode confinement varied from lot to lot with the placement of the oxide stripe. It was felt that the addition of the substrate confinement would substantially improve the reproducibility.

The TJS structure has previously been demonstrated by Kumabe et al.[2] The major modification planned in this program was to include a semi-insulating GaAlAs layer at the substrate interface to reduce current leakage into the GaAlAs confinement layers. Though this device has demonstrated most of the required characteristics for this program, continuous operation over a wide range of currents above threshold has also been demonstrated. The reliability of this structure is also not tested. For these reasons the TJS structure was given lower priority in the program than either of the others.

The self aligned structure shown in Fig. 1.1.3 was not originally proposed in this program but was later added to increase the options for success. The structure has many of the same features as the channeled substrate planar device developed by Hitachi. Confinement of both the mode and the current is accomplished by the interposition of the GaAs n-layer in the GaAlAs confinement

Figure 1.1.1. Schematic cross section of TJS laser structure.

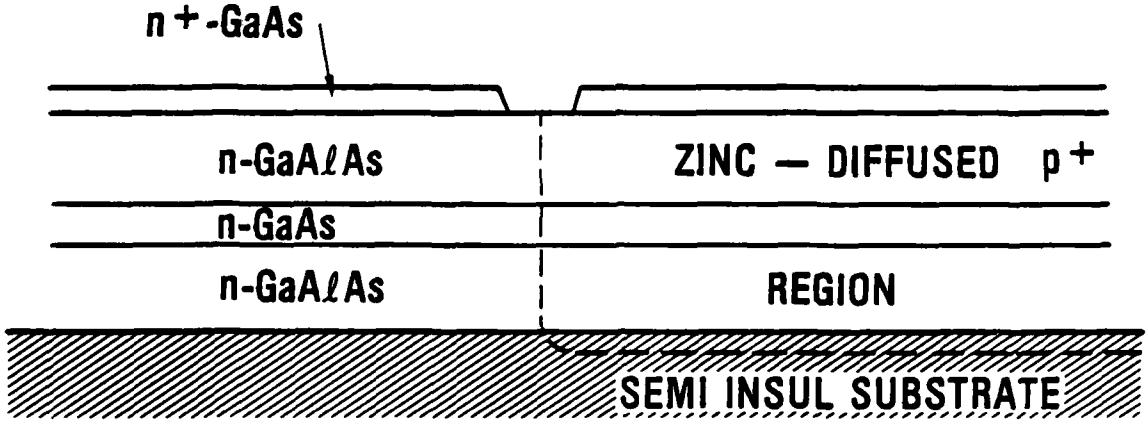

TJS STRUCTURE

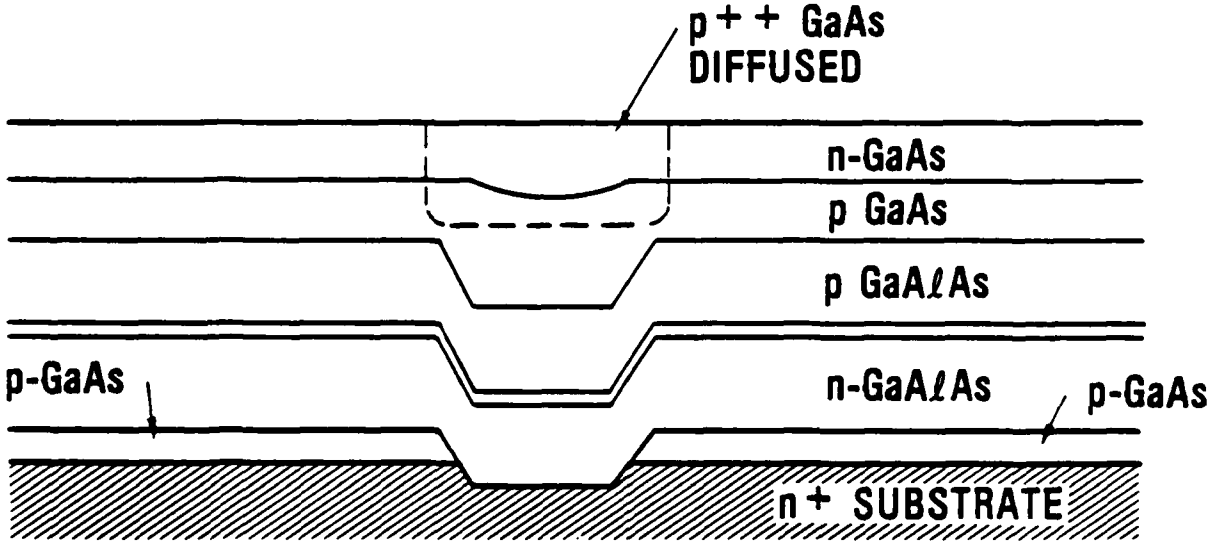

CHANNEL GUIDE STRUCTURE

Figure 1.1.2. Schematic cross section of channel guide laser structure.

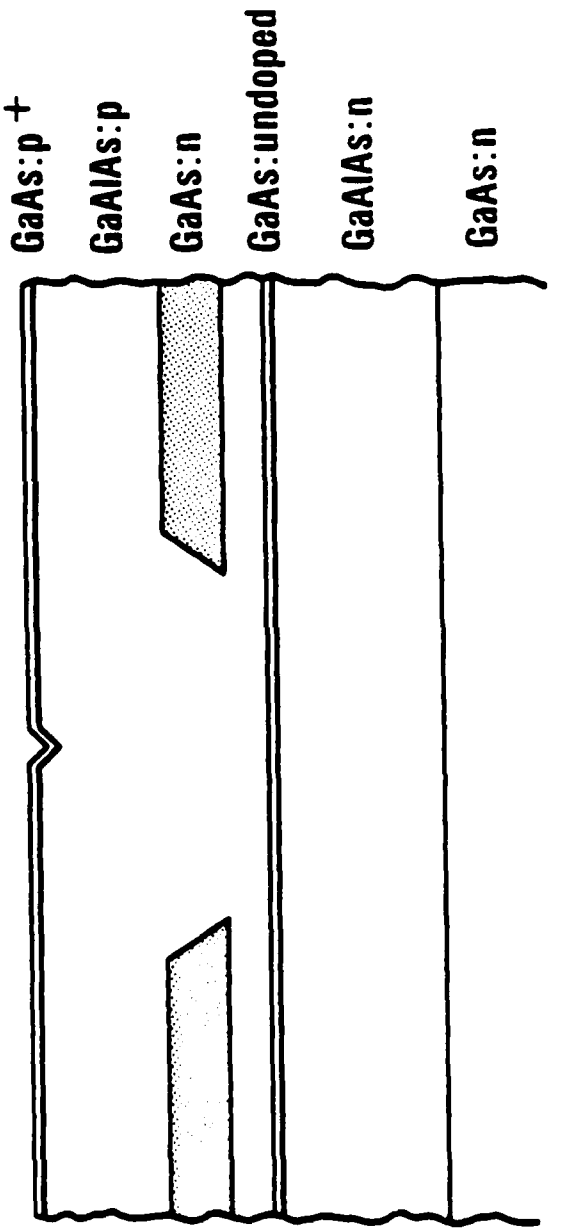

Figure 1.1.3. Schematic cross section of self aligned laser structure.

layer. The mode confinement is caused by the index step at edges of the interposed layers and the current confinement is caused by the presence of the back-biased junction. This device was chosen for inclusion when the pecularities of MOCVD growth made the realization of low threshold single-mode channel-guide lasers impossible to achieve. The self aligned structure became the device structure which most closely satisfied the needs of the Navy and was used for all deliverables.

1.2 Device Packaging

Effort was included in this program to develop a hermetically sealed fiber pigtail package for these devices. The basic philosophy was to develop packages which could be assembled and sealed with a minimum of "art." Initially the pigtails were to be graded-index multimode fibers. The problems associated with utilizing a manufacturable technique for the pigtail packaging of devices with single mode fibers were to be assessed.

The basic packaging concept was based on a nonactive process for aligning the pigtail to the laser. The concept employs preferentially etched grooves in Si as the alignment vehicle, as shown in Fig. 1.2.1. The laser is mounted on a Si submount into which a preferential groove is etched. Preferential etches with 100:1 or better plane selectivity have been developed for Si. This offers the possibility of having an alignment groove which is photolithographically positioned and which is defined by crystalline planes in the Si submounts. A technique similar to this has been utilized by workers at IBM for aligning arrays of lasers to fibers.

The subsequent bonding of the fiber to the can to provide the hermetic seal was to be accomplished by crimping or soldering. The finished package will be a coaxial TO-5 studded package. Rockwell's Interconnect Systems developed the package sealing technology.

1.3 Program Outline

To accomplish the development described above the program was organized into four tasks:

DEVICE PACKAGING STUDY

DEVICE SUBMOUNT CONCEPT

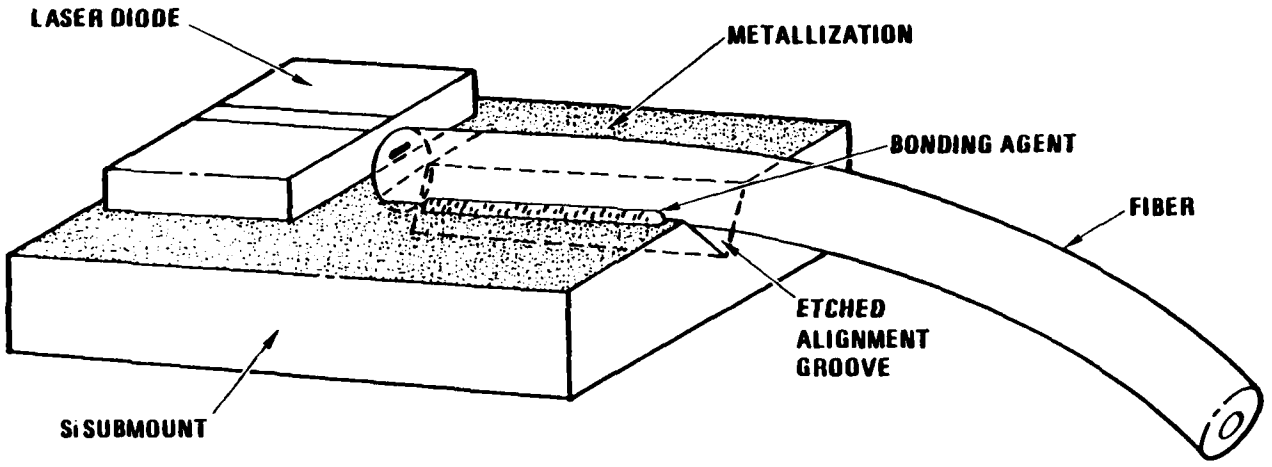

Figure 1.2.1. Schematic of device-submount fiber pigtail structure.

Rockwell International

Task 1 Device Design

Task 2 Device Development

Task 3 Device Testing

Task 4 Device Packaging.

The details of the developments undertaken and the results obtained will be discussed in Section 2.0. In Section 3.0 a summary of the program will be given and suggestions for future work are discussed in Section 4.0.

2.1 Task I - Device Analysis

The accurate analysis of the device structures to be investigated in this program provided guidance to the experimental work by determining the ranges of values suitable for single mode operation for both the device structures under consideration. In order to adequately calculate the regions of single-mode operation, it is necessary to analyze the electromagnetic mode properties of models for the waveguides for the two devices. This is then followed by calculations of the effective gain at threshold as a function of device parameters. These calculations provide the necessary determination of device parameters that result in ranges of operation in which the fundamental single mode operation dominates. Because the TJS and self aligned structures have been analyzed to some extent in the literature, and the device structures proposed in this program do not deviate greatly from that reported in the literatures, little analysis of these device structures was undertaken.

2.1.1 Five-Layer Dielectric Waveguide

The design problem of greatest difficulty for this program is the design of channel or bent guide structure. Although a variety of curved guide structures have been analyzed in the literature, none are close approximations to the channel guide structure, and as a result this is where the majority of the emphasis in the program will and has been devoted. The transverse perpendicular mode problem for channel guide structure and the other structures, for that matter, are similar and can be modeled as a five-layer dielectric. In addition, the channel guide structure may also be approximated as a five-layer dielectric for the transverse parallel mode distribution, if appropriate parameters for the bent portion of the guide can be derived. As a result, the problem of a symmetric five-layer dielectric guide was solved. Figure 2.1.1 shows the waveguide structure used in the calculations.

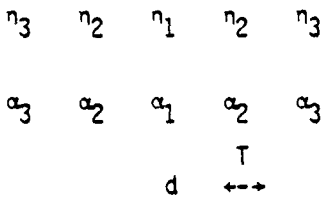

Fig. 2.1.1

Following the usual formula for propagating waves and multilayer dielectrics, the following eigenequation for the propagation constant was derived:

$$\tan \frac{h_1 t}{2} = \frac{h_2}{h_2} \frac{h_3 \cos (h_2 T) - h_2 \sin (h_2 T)}{h_2 \cos (h_2 T) + h_3 \sin (h_2 T)} \tag{1}$$

where

$h_i^2 = k_o k_i + \gamma$ and $k_i = k_i' + ik_i''$

$k_i' = n_i$ where n_i is index of refraction of the i^{th} layer and

$k_i'' = n_i \alpha_i / k_o$ where α_i is the net absorption (gain) coefficient of the i^{th} layer.

Equation 1 can be solved numerically for the propagation constant, γ, and the field distributions can then be calculated in each of the layers. Once Eq. (1) is solved for the propagation constant, this allows the calculation of the various field distributions in each of the layers. The program for calculating these field distributions can be used to calculate any five-layer dielectric guide. The problem then becomes establishing an appropriate model for a particular dielectric guide, so that parameters for a five-layer dielectric model can be determined. The major problem in the analysis of the bent guide structure is the development of an analytical model to determine these dielectric waveguide parameters. A variety of analytical models have been considered.

These are, for example, the models of Butler for gain guiding, the bent guide of Thompson and Henshell, and an additional model in which the bent waveguide region has been treated as a semicircular segment of a cylindrical guide. The gain guiding model and the bent guide model of Thompson and Henshell were significant deviations from the channel guide structure to be investigated in this program, and as a result a decision was made not to investigate those models for the present situation. The cylindrical segment model was treated in some detail by transforming it to a planar guide using conformal mapping. This model was felt to provide a reasonable approximation to a very narrow channel guide in which the guide itself would begin to approximate a semicircular region. However, the ends of a semicircular guide when transformed into a planar guide always resulted in a large abrupt dielectric discontinuity. This dielectric discontinuity was too large to adequately approximate the channel guide situation, and, in fact, the calculations for the cylindrical guide consistently yielded multiple mode configurations even for very narrow, i.e., very small radius, guides. As a result, it was felt that this model did not accurately represent the true situation in a channel guide structure, and it was abandoned.

2.1.2 Channel Guide Model

The schematic diagram of the model chosen for study is shown in Fig. 2.1.2. The waveguide properties and laser threshold conditions for this structure are analyzed based on the effective index of refraction model similar to that described by Aiki, et al,[3] for the channel substrate planar structure. The channel guide is treated as a five layer dielectric guide. Region I is the channel region. Regions II are the bent regions, and Regions III are the flat regions. An effective index of refraction must be determined for the bent regions of the guide.

For Regions I and III, the effective indices of refraction n_j' and loss coefficients α_j for the guide are determined from the propagation constant β_j' of an infinite planar guide

$$n_j' + i\frac{\alpha_j'}{2k} = \beta_j'/k$$

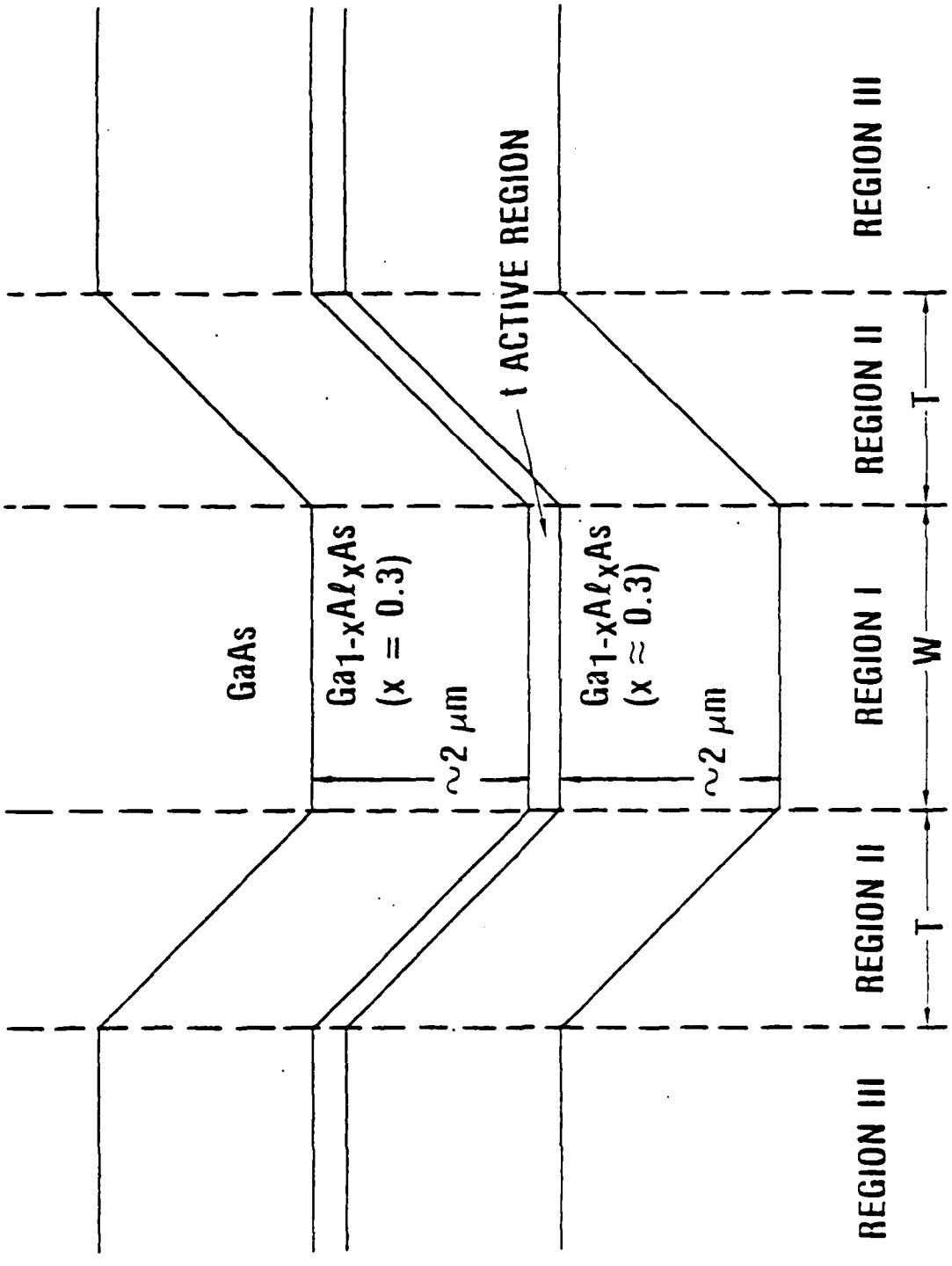

Figure 2.1.2. Channel guide five-layer dielectric model.

where $k = 2\pi/\lambda$ and λ = vacuum wavelength. Each region is treated as an infinite guide, and the propagation constant is derived as described above.

The propagation constant in the bent guide Region II is obtained by conformal mapping. These regions are also treated as infinite planar dielectrical guides and transformed to the appropriate angle by the following transform

$$W = u + iv = e^{-i\delta}(x + iy)$$

$$= (x \cos \delta + y \sin \delta) + i\,(y \cos \delta + x \sin \delta)$$

where δ is the angle of the portion of the bent guide. The propagation constants are determined by a solution of the regular five layer guide.

The propagation constants determined from solutions for Regions I, II, and III are then analyzed to determine an effective index of refraction and loss coefficient for each of the sections. These are, in turn, used in a solution of the five layer dielectric problem shown in Fig. 2.1.2, where the Region I represents the active regions, II the bent guide and III the surface guide. This, of course, is an approximation which ignores the physical bend which must be accommodated at the interfaces of the various regions. However, these abrupt bends are thought to provide further losses for higher order modes. So, the calculations represent a worst case solution. Representative calculations of the intensity distribution in the guides are given in Figs. 2.1.3 and 2.1.4 for different values of the guide properties. The calculations show conditions in which the fundamental mode (Fig. 2.1.3) for a channel width of 2 μm or first order mode (Fig. 2.1.4) for a channel width of 5 μm are possible.

The above procedure can now be used to determine the modal characteristics of any channel guide structure. In particular, the parameters for the fundamental transverse parallel mode and the first order transverse parallel mode can be determined. The indices of refraction and attenuation constants for each transverse region are determined and used in a calculation of the threshold gain as detailed below. The basic condition for threshold is that the sum of all gains and losses in the dielectric structure be equal to zero. To calculate the

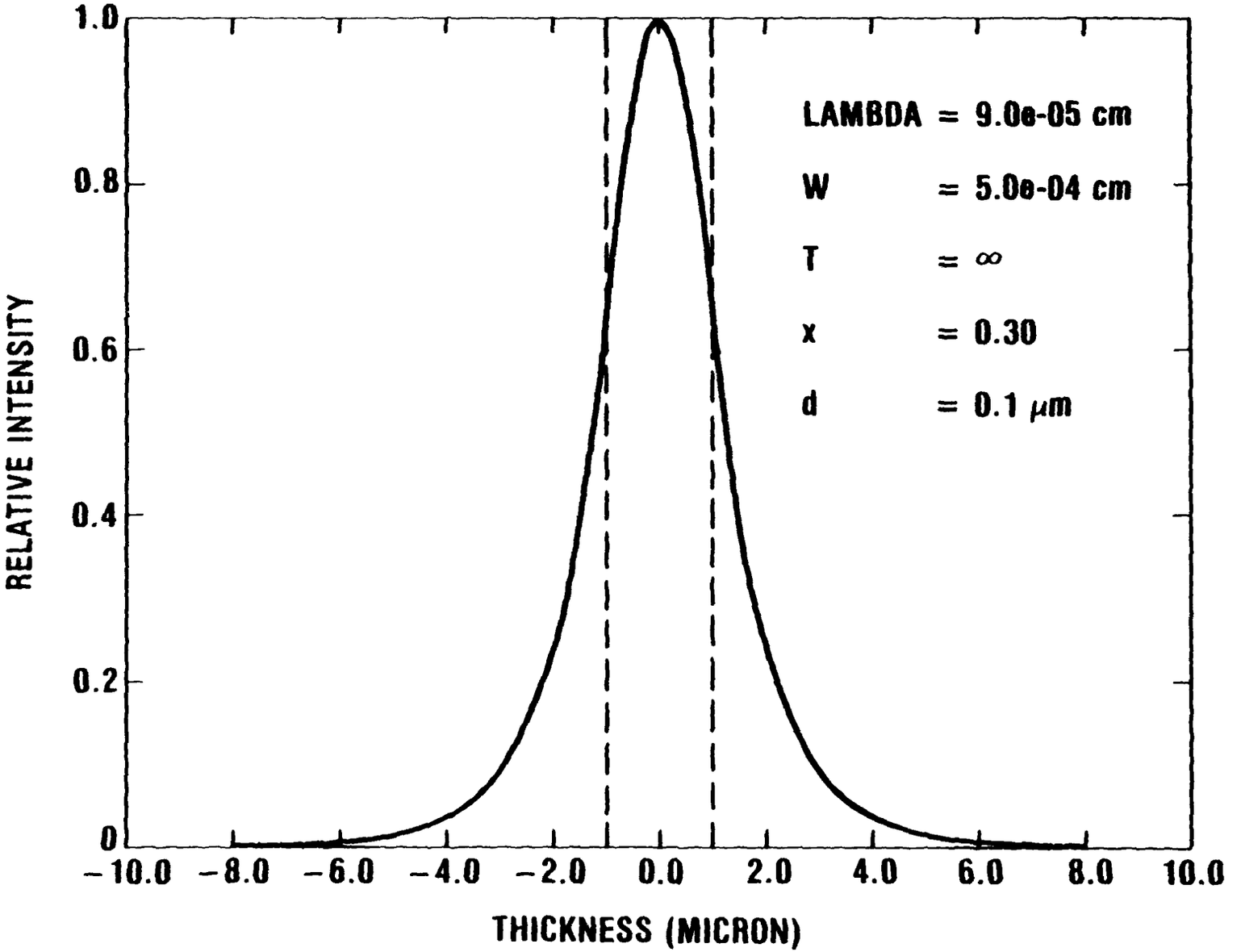

Figure 2.1.3. Intensity distribution for fundamental mode.

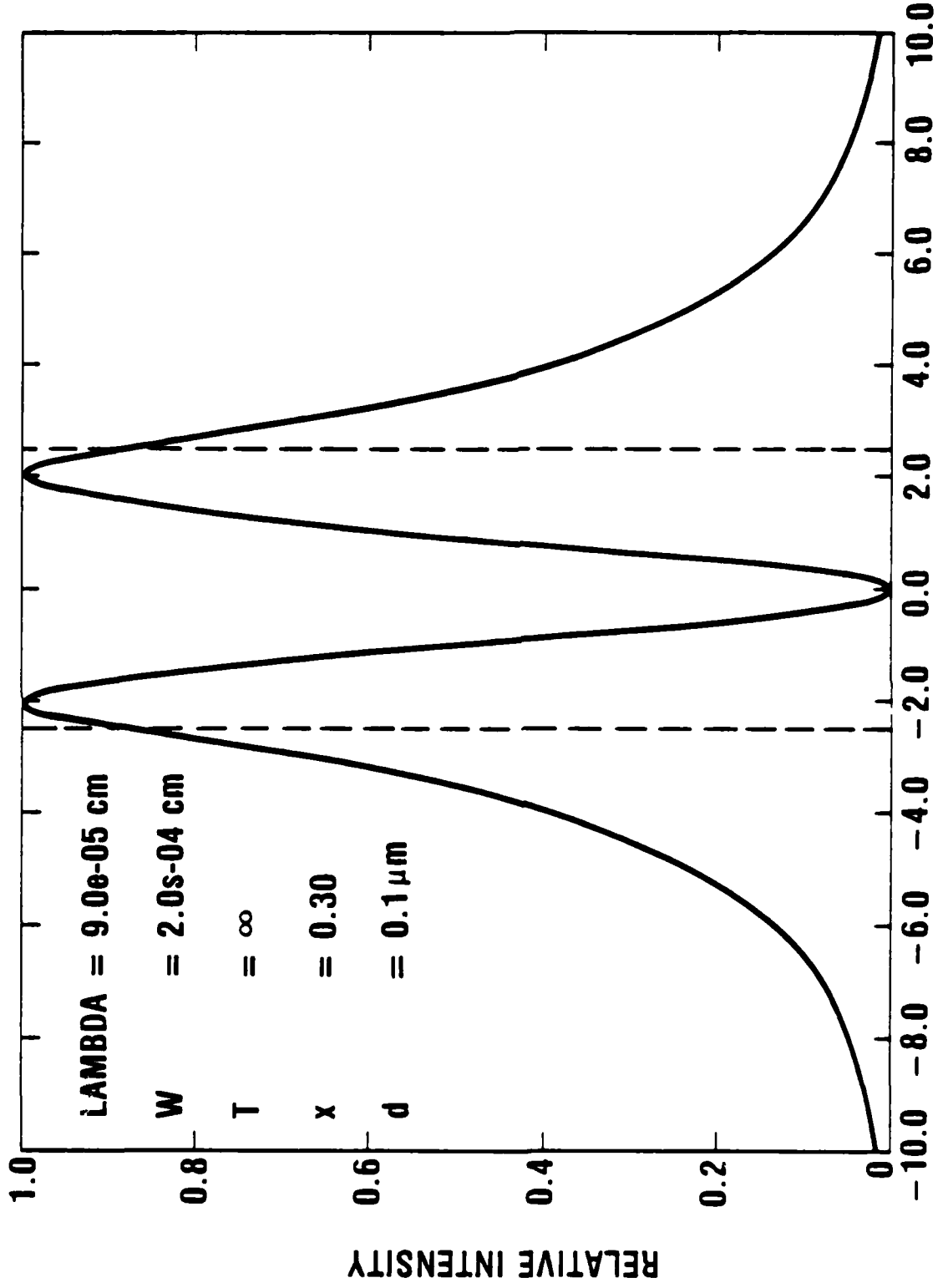

Figure 2.1.4. Intensity distribution for first-order mode.

threshold gain then, we use the following equation

$$\Gamma g_{th} = \sum_{i=1}^{3} a_i \alpha_i + L^{-1} \ln (R^{-1})$$

where the a_i can be written as

$$a_i = \int_i E^2 (x)\, dx$$

where $L^{-1} \ln(R^{-1})$ is the loss due to the reflectivity of the laser mirrors. The a_i are the field strengths in the various regions of the cavity. $\alpha_1 \equiv \alpha_{fc}$ is due to free carrier loss in the active region. The confinement factor, Γ, is the field strength in the active region. Therefore $\Gamma = a_1$. By recasting this equation, one can develop an expression for the threshold gain, g_{th}

$$\Gamma g_{th} = a_2\alpha_2 + a_3\alpha_3 + \Gamma\alpha_{fc} + L^{-1} \ln (R^{-1})$$

In all subsequent calculations, we have let the quantity, $\Gamma\alpha_{fc} + L^{-1} \ln(R^{-1}) = 45\ cm^{-1}$. The confinement factor and the various field strengths in the regions are determined from the effective indexes of refraction of the regions of the channel guide. Similarly, the attenuation constants for the regions of the channel guide other than the active region are determined from an analysis of this structure.

The threshold gain is obviously a function not only of W, the width of the active region, and T, the width of the bent regions of the guide, but is also a function of t, the thickness of the active layer, and also the thickness of the GaAlAs confining layers. We have undertaken a systematic variation of these parameters and calculated the threshold gain for various values of the active region width, W. Figure 2.1.5 shows the variation of the fundamental mode threshold gain with the width of the active region, W, for three different values of the width of the bent regions of the guide, T. Note that there are only minor differences in the dependence of the threshold gain on active region width for any of the values of T. As a result, in all subsequent calculations, we have chosen $T = \infty$ to simplify the calculations.

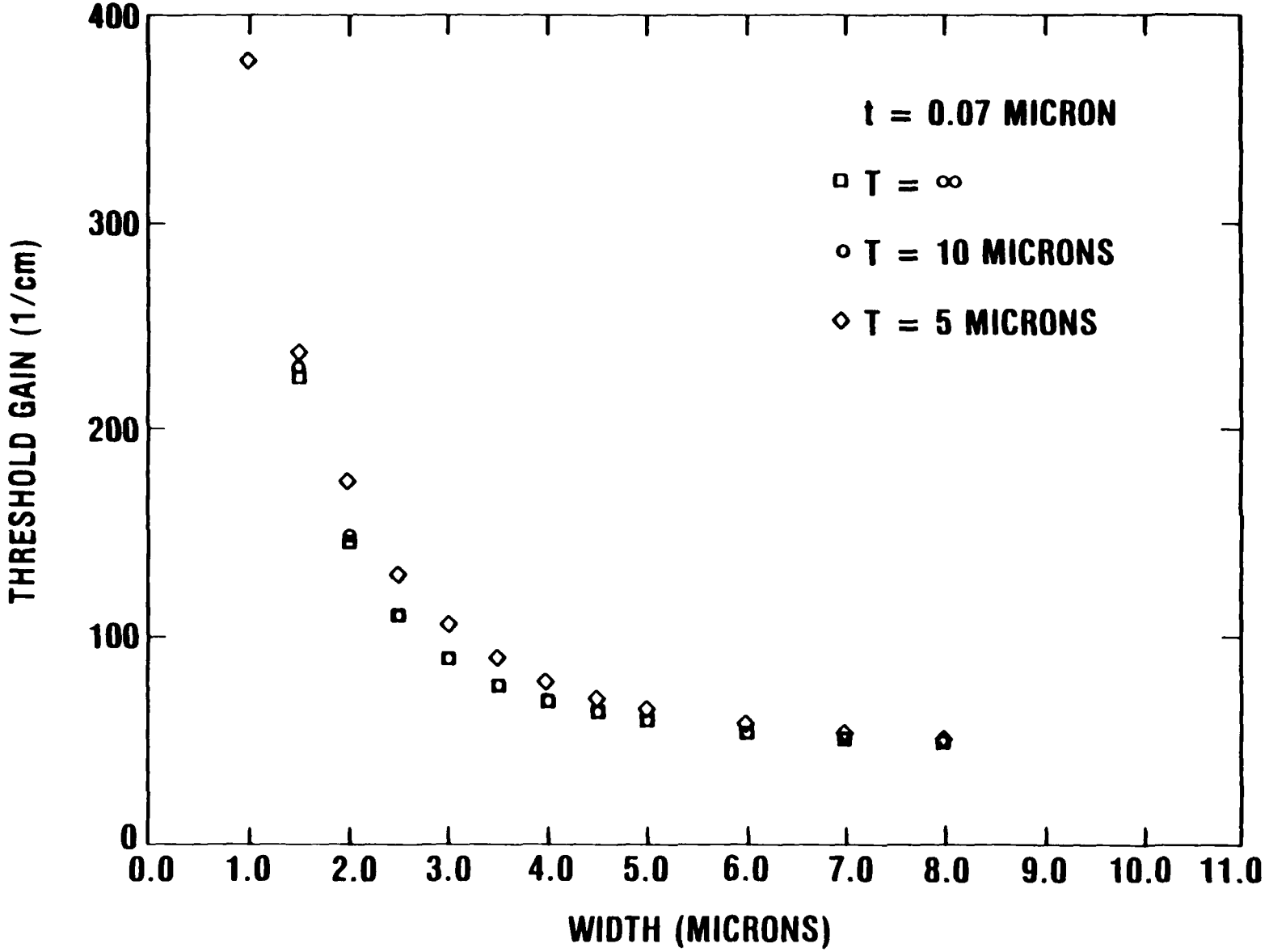

Figure 2.1.5. Threshold gain versus channel width for various T.

Figure 2.1.6 shows the dependence of the threshold gain on active region width for both the fundamental mode and for the first order mode in a channel guide laser structure. These calculations were performed for an active region thickness of 1000A. The threshold gain for the fundamental mode is independent of the width of the active region down to a channel width of approximately ~ 1.5 μm. At this point, the threshold gain increases steeply with further decreases in the width of the active region. Similarly, the first order mode first shows a relatively weak dependence upon active region width down to an active region width of ~ 5 μm. Below this width, the gain for the first order mode increases strongly with decreases in the active region width. Therefore, one can define a range of active region widths over which only the fundamental mode will be possible in a channel guide structure. For the device structure of Fig. 2.1.6, this range of widths extends from approximately 1.5 μm to 5 μm. Within this region, the device should operate in stable single transverse and longitudinal mode.

This analysis now allows one to calculate similar sets of curves for variations in the waveguide parameters of the channel guide structure. For example, the active region thickness is expected to determine to a large extent the width of the channel guide over which a single mode operation can occur. From the data presented here the maximum channel width as a function of active region thickness for 30% confining layers can be calculated and is shown in Fig. 2.1.7 by the dashed curve. Other considerations, however, are important in determining the channel width in our device design. For example, a constraint of major concern is that of achieving a threshold current of 25 mA or less. To calculate the stripe width necessary to achieve a threshold of 25 mA for a 400 micron long device, we have used the theoretical formalism used in a paper by Dupuis and Dapkus. In that work, the threshold current density as a function of active layer thickness was calculated for a variety of Al concentrations in the confining layers. The use of the theoretical curves generated in that work and the constraint of a 25 mA threshold current we have generated the upper solid curve in Fig. 2.1.7, labeled theoretical. This curve then represents the locus of stripe width at a particular active region thickness which will result in a threshold current of 25 mA. Stripe widths larger than this solid line will

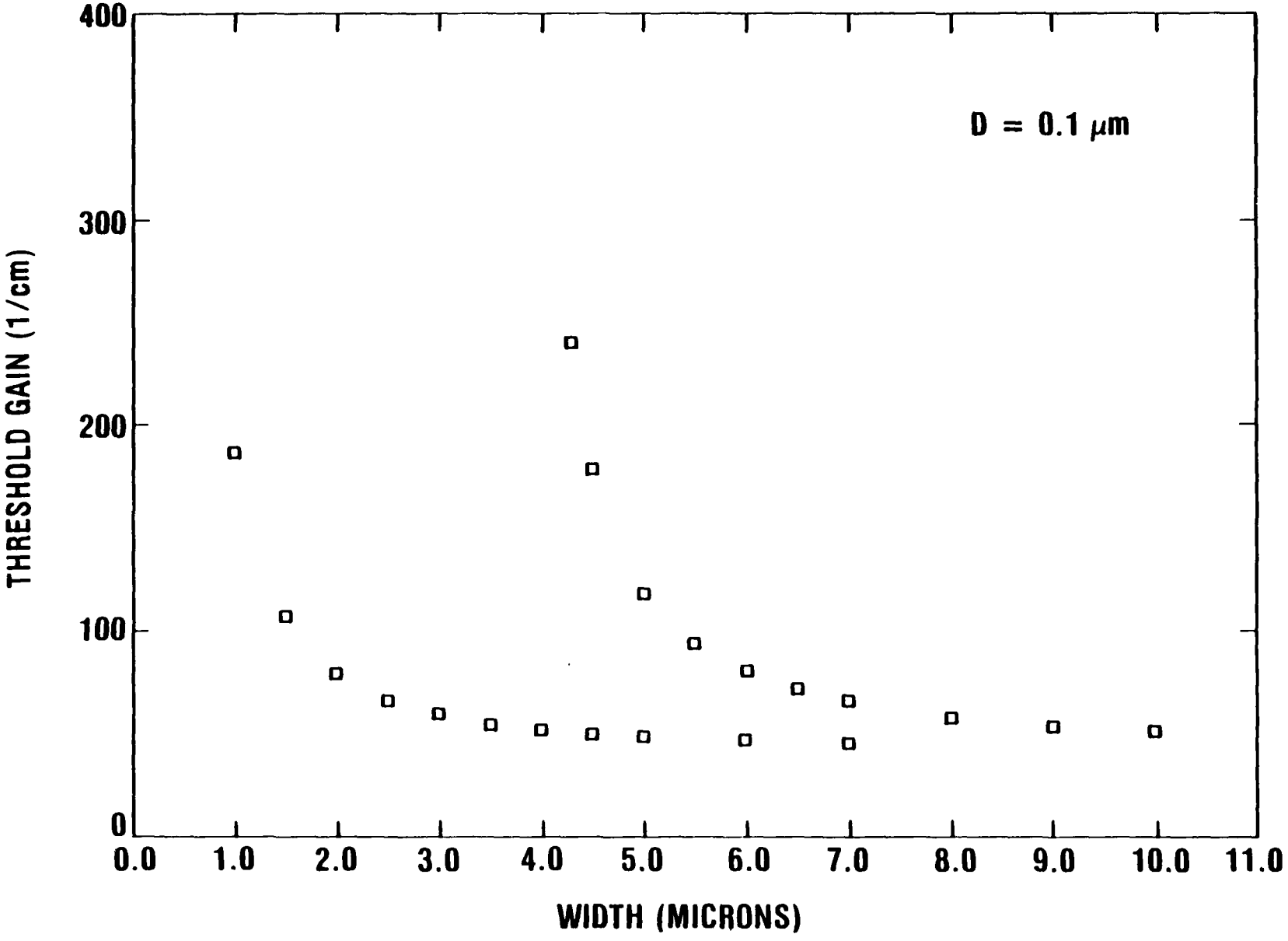

Figure 2.1.6. Threshold gain versus channel width for fundamental and first order mode.

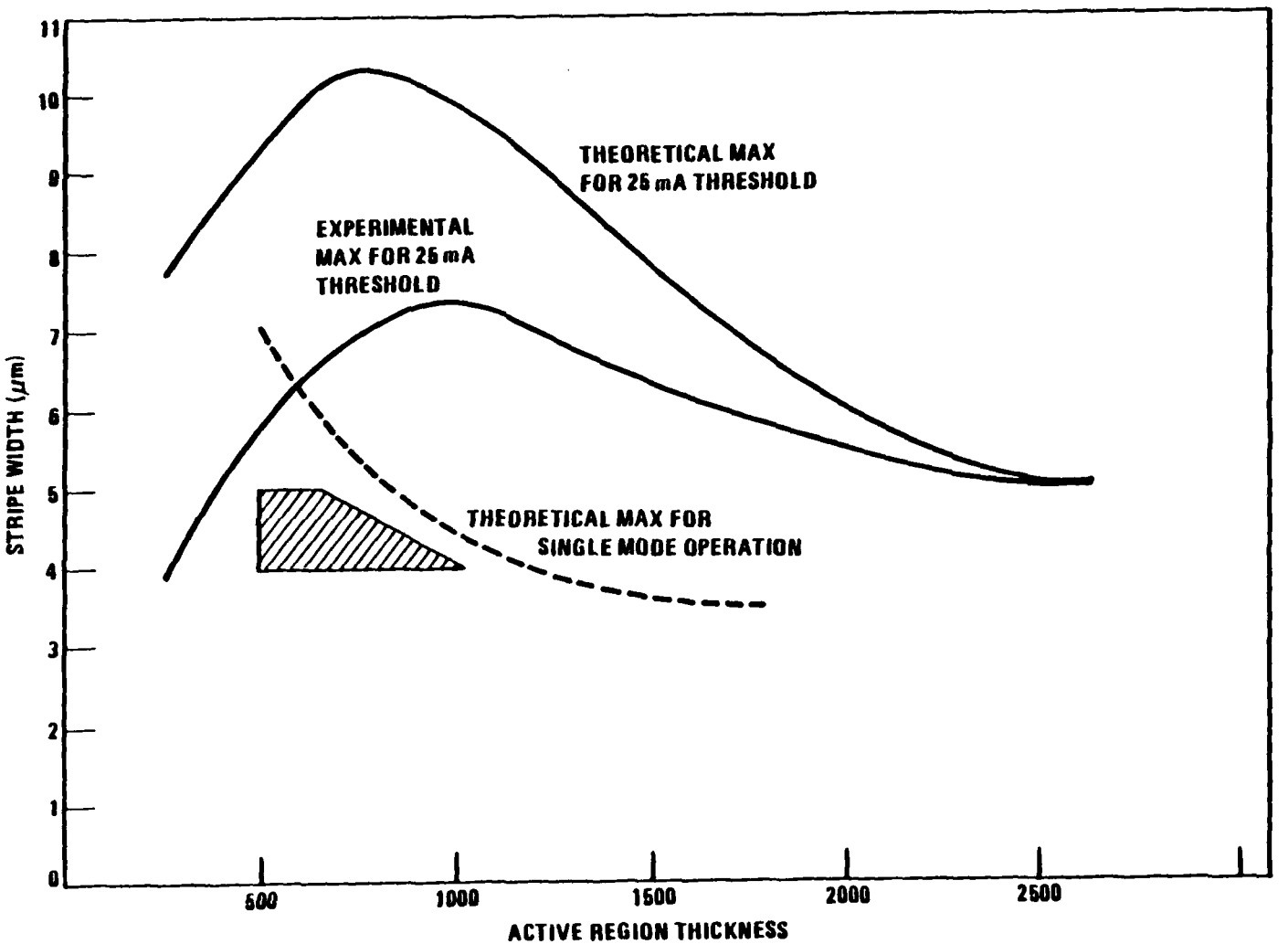

Figure 2.1.7. Channel width versus active region thickness.

result in higher threshold currents, and stripe widths lower than this theoretical curve will generate threshold currents below 25 mA.

The second solid curve in Fig. 2.1.7 labeled experimental is the locus of experimental data points generated in the work by Dupuis and Dapkus showing the actual dependence of experimental devices. This curve represents the realistically achievable thresholds for broad area devices. It does not take into account expected losses of current resulting from current spreading. However, because of the use of a reverse bias junction both at the bottom and at the top of the stripe, it is felt that the current spreading will not be great. At most this should represent approximately a 15% increase in the threshold current.

Combining the dashed curve for the waveguide properties of the laser with the experimental curve for the threshold current density, we have estimated that the appropriate device parameters for the channel guide structure lie within the region shaded in Fig. 2.1.7. A lower limit of 4 microns was placed on the stripe width for the channel guide laser to improve photolithography yield and to minimize the problems of growth in very narrow channels. From this analysis, it would appear that an active region thickness in the range of 500 to 1000A and a stripe width of somewhere between 4 to 5 microns represents a reasonable engineering estimate of the appropriate device parameters.

2.1.3 Transverse-Junction-Stripe Model and Parameters

The transverse-junction-stripe geometry (TJS) laser[4-6] has been under investigation for some time. Although the first TJS structures had single-longitudinal-mode emission characteristics and low threshold currents at 23°C, the threshold current density showed a strong temperature dependence that resulted in an increase in I_{th} by a factor of 65 from room temperature to 70°C. A different TJS structure has been reported that has greatly improved J_{th} vs T characteristics with CW I_{th} values as low as 27 mA.[7] The structure is produced by growing four layers alternating between n-type GaAs and n-type GaAlAs on a semi-insulating GaAs substrate. A p^+ Zn-diffused region is then formed in one half of the device using a Si_3N_4 stripe masks. This p-region extends into the semi-insulating substrate. A channel is formed along the top of the device

by etching away a strip in the top n-GaAs layer where the p-n junction intersects the top of the wafer, thus isolating the top diffused p-GaAs region from the top n-GaAs region. The p- and n- contacts to the device are made respectively to these regions.

The active region in this structure is defined by the central GaAlAs-GaAs-GaAlAs heterojunctions on one side and the extent of carrier diffusion at the central GaAs p-n junction. Note that in this structure, the active electrical junction is normal to the GaAlAs-GaAs heterojunctions and that this device is actually a GaAs homojunction laser. Because the GaAlAs p-n junctions also formed by the Zn diffusion have a higher forward voltage, minority carrier injection occurs primarily at the GaAs p-n junction. However, optical and carrier confinement normal to the junction is provided by the GaAlAs-GaAs heterojunctions. Thus, in this TJS structure, transverse-parallel mode confinement is provided by the index discontinuities at the central heterojunctions. The stabilization of the transverse-perpendicular mode is the result of gain guiding along the GaAs homojunction active region. The "width" of the active region is set by the heterojunction spacing while its "height" is determined by the minority carrier diffusion lengths in the GaAs homojunction region. Because the GaAs p and n layers are heavily doped with p-1 x 10^{19} cm^{-3} and n-2 x 10^{18} cm^{-3}, this "height" is 1 - 2 μm. This structure is expected to provide stable single transverse parallel and transverse perpendicular cavity mode operation for a wide range of CW currents.

Such performance has indeed been demonstrated with single-mode operation up to twice the threshold current at output powers greater than 4 mW per mirror. CW operation at temperatures up to 110°C has also been reported.[6] Recent information indicates that lifetimes of 10^4 hours at room temperature and values of I_{th} = 25 mA are achievable with TJS devices.[7] An improved version of the TJS structure was designed for this program. This ITJS laser structure employs an SiO_2 mask that passivates and protects the p-n junction in this region as well as permitting the bonding of the metal contacts directly to a header that has specially-prepared contact bond pads. TJS diodes with the previously described structure have to be mounted in a junction-up configuration using conventional Au-wire bonded lead contacts.[4] Consequently, the heat

sinking is poor. This results in excessive heating during CW operation and a corresponding large shift in the emission wavelength as a current is increased.

The SiO_2 passivation offers other advantages that would potentially be important in numerous applications. This mounting technique results in a more reliable device for two reasons: (1) the fragile flexible bond wires are eliminated leading to a more rugged package, and (2) damage introduced in the laser chip itself during the bonding operation are eliminated. In addition, this structure affords simple hybrid connection to Si laser driver integrated circuits and integrated optical components using the Si wafer itself as a heat sink. While bonding of this type was not attempted in this program it remains an attractive feature of the device.

Another unique feature of the proposed improved ITJS structure is the reduction of shunt currents at high drive currents (high forward voltages) and high temperatures.[33] This is accomplished by making the $Ga_{0.6}Al_{0.4}As$ confining layer that is grown on the semi-insulating substrate a semi-insulating epitaxial (but n-type) $Ga_{09.6}Al_{0.4}As$ layer. Thus, we call this the insulated TJS (ITJS) structure. Such semi-insulating layers are not readily grown by LPE because of the $n\text{-}10^{16}$ cm^{-3} doping level background typically observed for LPE-grown GaAlAs films. However, we demonstrated that such high-resistivity GaAlAs films can readily be grown by MO-CVD. The use of a semi-insulating $Ga_{0.6}Al_{0.4}As$ layer instead of a highly-conducting one, results in the elimination of the shunt current that flows through the diffused p-n junction in this layer. This current can be detrimental to laser performance at high currents and at high temperatures.[5] This results in a reduction of the shunt current in the device by a factor of 2 and as a result, in improved high-temperature performance of ITJS lasers.

In the ITJS devices developed for this program, the $Ga_{1-x}Al_xAs$ active layer composition can be x-0.1 to provide single-frequency output at λ-8200Å to capitalize on the low losses that occur in most fibers near this wavelength. While most of ERC's laser development has been for DH devices with GaAs active regions, low-threshold DH lasers with $Ga_{1-x}Al_xAs$, x-0.1 active layers have been

grown by MO-CVD. The approximate values of layer thicknesses, doping levels, and alloy compositions of the ITJS structure are given in Table 2.1.1.

Table 2.1.1
Details of the ITJS Structure

Layer No.	Composition	Thickness (Microns)	Doping Level (cm^{-3})
1	$Ga_{0.6}Al_{0.4}As$:Undoped	~1.0	High Resistivity
2	$Ga_{0.9}Al_{0.1}As$:Se	~0.3	$n = 2 \times 10^{18}$
3	$Ga_{0.6}Al_{0.4}As$:Se	~1.0	$n = 2 \times 10^{18}$
4	GaAs:Se	~0.6	$n = 6 \times 10^{18}$
Substrate	GaAs:Cr	~100	High Resistivity

2.1.4 Structure Optimization for Program

Once the preliminary detailed analysis of the channel guide structure and the transverse junction stripe structure was completed, experimental work on both structures began in earnest. While fundamental structural and electronic features of the two laser devices can, in principle, be determined theoretically, the actual devices require some flexibility owing to less obvious experimental phenomena. In particular, device processing limitations require some modification of theoretically determined device structures. For these reasons the device development portion of this program proceeded from the starting point of the theoretically determined structure toward more experimentally practical devices. This evolution is described in Section 2.2 below.

2.2 Task II - Device Development

Experimental development of the two primary single mode laser structures analyzed in the preceding section began by taking advantage of previous Rockwell experience in the growth of high quality MO-CVD epitaxial layers for optical source applications. Some additional materials growth studies and

device processing techniques were developed specifically for this program. In addition, the device structure itself, in the case of the channel guide laser, underwent significant evolutionary development owing to processing requirements and limitations. The final and intermediate stages of these devices are described in detail in this section.

2.2.1 Materials Growth

The multilayered $Ga_{1-x}Al_xAs$-GaAs heterostructure wafers required for the fabrication of devices in this program were grown by the metalorganic chemical vapor deposition (MO-CVD) process. As applied to the growth of III-V compounds and alloys the MO-CVD process involves the mixing of a metal-organic compound of a Group III element with a hydride or metalorganic compound of a Group V element, and pyrolysis of this mixture or its reaction product under appropriate conditions to produce the Group III-Group V semiconductor. Thus, for example, trimethylgallium (TMGa) and arsine (AsH_3) are mixed at room temperature in a cold-wall reactor to form GaAs according to the following simplified equation:

$$(CH_3)_3Ga + AsH_3 \xrightarrow{\Delta} GaAs + 3CH_4$$

by mixing TMGa in the gas phase with trimethylaluminum (TMAl) and AsH_3, GaAlAs is obtained upon pyrolysis at established temperatures; the composition of the alloy is controlled by the ratio of the reactants. The organic byproduct, methane (CH_4), is stable at film growth temperature.

The deposition occurs by passing a homogeneous gas mixture of reactants, dopants and carrier gases over a heated substrate. Only the temperature of the substrate need be controlled. The partial pressure of the various gaseous constituents can be controlled by electronic mass flow control of the flow rates of the various gases. These features allow all the critical variables in the growth process to be controlled with extremely good accuracy, thus ensuring reproducibility.

The reactors used in the proposed program have facilities for several metalorganic sources, dopants and Column VI hydrides. These various gases are switched into the reactor chamber at the appropriate time under complete microprocessor control. In addition, the MO-CVD process involves no etching species so that abrupt interfaces between various materials are expected. The absence of an etching species also helps to achieve the growth of films with uniform thickness and composition, since the growth process is not the result of competing deposition-etching reactions. Such reaction could lead to the introduction into the gas phase of uncontrollable amounts of III-V compounds substrate components, which would subsequently upset the desired film stoichiometry and impurity level.

The metal alkyls TMGa, TMAl, and DEZn are liquids at the source temperatures typically employed. H_2 gas is bubbled through the liquids and the reactant vapors are mixed with AsH_3 and pyrolyzed at or near the substrate. The alloy composition of GaAlAs films is determined by the ratio of the initial TMGa/TMAl partial pressures. The p-type Zn and *n*-type Se doping levels are similarly controlled by the initial partial pressures of DEZn and H_2Se, respectively. Layer thicknesses are controlled by the timed sequencing of the appropriate reactant flow-path control valves.

The structures required for stable single-mode operation critically depend on precise control of doping, alloy composition, and layer thickness for optimum performance and the reproducible realization of the device characteristics. Excellent uniformity of these three important material and structural parameters has been demonstrated. This uniformity across a substrate yields a similar high degree of uniformity in the performance characteristics of lasers fabricated from MO-CVD DH wafers.

The unique growth characteristics of the MO-CVD process have been a key element in the development and demonstration of the channel-guide and self aligned single-mode lasers. In fact, these structures would be difficult, if

not impossible, to grow by liquid phase epitaxy (LPE) because the difference in the chemical nature of growth on the (111) and (100) planes that is characteristic of LPE would produce continuously curved, concave active regions that result in DH lasers that do not stabilize the tansverse-parallel cavity mode.

2.2.2 TJS Studies

The fundamental issues in the development of TJS devices are the Zn diffusion that forms the laser active region and subsequent multistep processing to form contacts. In addition, diffusion studies for stripe definition of channel guide structures is a byproduct of TJS diffusion studies.

The TJS structure was considered an alternate structure in this program. While an attractive device design, its reliability at the required power output levels was considered questionable.

We decided to pursue the use of spin-on doped oxide diffusion sources for stripe definition. These sources are under reasonable control by the manufacturer and are much simpler to deposit and use than conventional nitride masking and diffusion. The latter requires plasma etching of the windows in the nitride which is difficult to control without damaging the GaAs surface. The oxide sources, however, can be deposited and etched off with HF acid. Sources were obtained from Emulsitone Corporation. The sources are basically emulsions which contain silicon dioxide and other sources of appropriate dopants such as zinc oxide. These emulsions are spun onto a wafer using standard photoresist spinning techniques and then baked at about a temperature of 130°C to densify the oxide to drive off any residual water vapor. This results in an oxide whose properties are adequate to serve as a source of zinc for subsequent heat treatment and diffusion. Several different sources of zinc doped spin-on oxides were obtained from Emulsitone including a proprietary source which was developed to reduce the amount of surface erosion that can occur with the use of these oxides and volatile III-V compounds such as GaAs and GaAsP or GaP. Experiments

were carried out to determine the temperature dependence of the diffusion depth for these sources over a range of temperatures that would be compatible with device processing. These experiments have resulted in the conclusion that the present zinc doped spin-on oxides are inadequate for use in this program. There are several reasons for this conclusion. First, the use of these oxides in an open tube system with no arsenic over-pressure results in serious erosion of the top surface of the crystal during the diffusion process. This erosion results in severe pitting and a morphology which is not compatible with subsequent device processing. Although this erosion was most severe at temperatures of 700°C and higher, it was present at all temperatures investigated and represents a major barrier to the use of these oxide sources. Experimentation was performed in a vertical CVD reactor where an over-pressure of arsine could be used to maintain the arsenic partial pressure at the surface of the crystal. These experiments, while improving the surface erosion considerably, were still inadequate to allow the consideration of these sources for this program. The second reason why these sources are inadequate is that the surface concentration of zinc yielded by these sources is too low for the purposes of this program. This was deduced by a measurement of the depth of diffusion for a specific time of diffusion as a function of the temperature at which the diffusion occurred. Even at temperatures as high as 700°C and for exceedingly long periods of diffusion in excess of 10 hours, diffusion depths of only approximately 1 μm were achieved in n^+ substrates of doping about $10^{18}/cm^3$. The times and temperatures required to achieve these diffusion depths were incompatible with the device goals of this program.

Because of disappointing results obtained with spin-on oxide dopant sources, our diffusion efforts were directed entirely toward closed-tube Zn diffusion utilizing Si_3N_4 masking techniques.

A station for the sealing of quartz ampoules for zinc diffusion was established in our Thousand Oaks Laboratories. Ampoules were designed for GaZn-As ternary diffusions. Preliminary experiments established 675°C as a suitable temperature for diffusion from a Ga-ZnAs-As source, and experiments were done to determine diffusion depth vs time for the conditions. Silicon nitride deposition techniques are well in hand from implantation annealing work and

plasma etching of the nitride is under reasonable control. Using this etched technique, several preliminary channel guide structures have been prepared.

The zinc diffusions for both the channel guide and the TJS structure must be performed through a mask to limit the area of diffusion. Figure 2.2.1 shows some of the difficulties that can occur for an improperly masked substrate. Shown here is an SEM photograph of a cross-section of a substrate with a diffused region. There are no epitaxial layers on the substrate. The difference in color between the diffused region and the nondiffused region is due to the voltage contrast between these two conductivity types. This diffusion was performed by masking a wafer with a sputtered silicon nitride layer approximately 2000A thick. This nitride was then removed in 8 micron stripe regions, and the wafer was then inserted in a closed ampoule and sealed with a solution of Ga containing zinc arsenide and arsenic. Early experiments indicated that the use of less than a sufficient amount of arsenic in solution will result in severe pitting of the unmasked portion of the wafer. As a result, these results were obtained with a large over-pressure of arsenic in the sealed ampoule. The diffusion was carried out at 675°C. Provided there is sufficient arsenic overpressure, no degradation of the top surface of the wafer is observed. However, a problem is evident in this photograph in the presence of substantial zinc diffusion along the surface of the wafer and subsequent diffusion into the wafer in regions well underneath the masked strip barrier.

Diffusions were also carried out on an optimum TJS structure. The TJS double-heterojunction structure upon which initial zinc diffusions were performed is as follows:

GaAs substrate: Si($n \sim 10^{18} cm^{-3}$)/~1 μm GaAs: (undoped, $n \sim 10^{18} cm^{-3}$) ~ 1.0 μm
$Ga_{0.7}Al_{0.3}As$: Se($n \sim 10^{18} cm^{-3}$)/~0.3 μm GaAs: ($n \sim 10^{18} cm^{-3}$)/~ 1.0 μm
$Ga_{0.7}Al_{0.3}As$: Se($n \sim 10^{18} cm^{-3}$)/~0.5 μm GaAs: Se ($n \sim 10^{18} cm^{-3}$)

A 1000A plasma deposited nitride is used as a diffusion mask. Stripes in the nitride mask were opened using an rf plasma etching system.

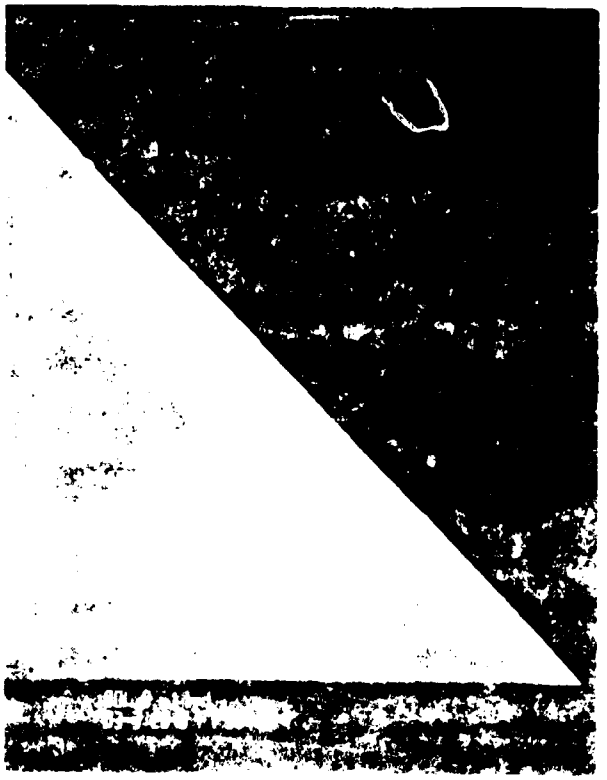

Figure 2.2.1. Zinc diffused TJS structure--improperly masked.

The ternary diffusion source used in this work contains gallium arsenic and zinc in the ratio of 77.2:18.7:4.1 atomic percent. The zinc and arsenic are in the form of Zn_3As_2 and are mixed with pure gallium and pure arsenic at 300K and placed into a quartz ampoule. Following insertion of the sample, the ampoule is evacuated to 2×10^{-6} Torr with an ion-vacuum pump and sealed. Various diffusion times have been tried, with a time of 130 minutes producing the best results for a diffusion temperature of T = 675°C. After diffusion the samples are sealed again in an ampoule with 10 mg arsenic and annealed at 900°C for 120 minutes. After removal from the ampoule, a non-uniform brush pattern was observed on the surface of some samples. The origin of this pattern is possibly oxidation of the surface or contamination from incompletely cleaned starting materials.

New handling procedures adapted to minimize these problems were: (1) the ampoule is cleaned in HNO_3:HF:H_2O (1:1:3) immediately before use, (2) Zn_3As_2 is employed as part of the diffusion source, (3) the surface is examined immediately prior to ampoule insertion, (4) HCl:H_2O (1:10) is used to clean the Ga prior to the addition of the Zn_3As_2, and (5) the Ga:ZnAs diffusion source ratio has been changed to 33.2:40.1:26.7 atomic percent. The first four steps should result in fewer unintentional impurities. Changing the Ga:Zn:As should provide more reproducible diffusion junction depth and profile.

The diffusion temperature has been increased to 700°C. For this diffusion temperature, 30, 65, and 120 minute diffusion times have been used. It appears that the 65 minute diffusion is optimum. The 30 minute diffusion results in a diffusion that is too shallow, while the 120 minute diffusion leads to excessive Zn diffusion along the nitride-GaAs interface and excessive lateral Zn diffusion into the AlGaAs layers. This is shown in the SEM photomicrograph of Fig. 2.2.2. Shown for comparison in Fig. 2.2.3 is the SEM photomicrograph of the 65 minute diffusion. In Fig. 2.2.3, Zn diffusion along the nitride-GaAs and lateral Zn diffusion in the AlGaAs layers is minimal.

Several initial devices were fabricated from the wafers described. The contact metalization for these TJS devices was evaporated Zn-Au for p-type material and Au-Sn-Pt for the n-type material utilized in conjunction with the

Figure [illegible]. Zinc diffused TJS structure--120 minutes.

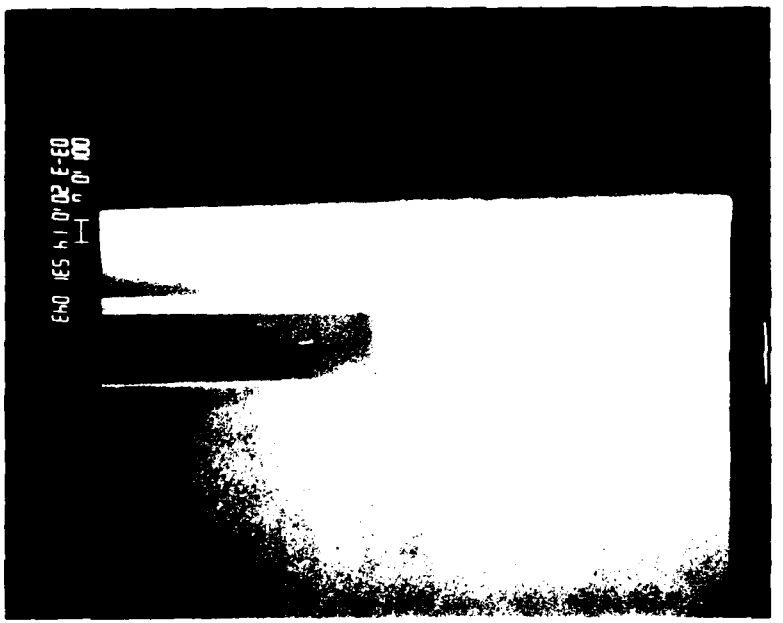

Figure 2.2.3. Zinc diffused TJS structure--65 minutes.

multilevel photolithographic mask set designed earlier. The devices are mounted junctions side-up on TO - 18 headers with silver epoxy. Thermocompression bonded wires are attached between the die and header post. On the initial wafers tested, the current threshold (I_{th}) was in the 200 mA range under pulsed room temperature operation. Single longitudinal operation was not observed for these devices. Possible causes for the high threshold current and multimode emission are current leakage through the substrate, low quality diffusion wafer and source preparation and non-optimum diffusion-anneal parameters.

At this point a decision was made that the program goals could best be met by devoting the entire experimental effort toward the channel guide structure and its successors.

2.2.3 Channel Guide Laser Development

Prior to the fabrication of actual channel guide laser devices, two important aspects of the device were studied. These aspects of the device are the processing and etching steps necessary to obtain high quality grooves and the electrical characteristics of the back biased p-n junction used to block current flow through all but the bent guide region of the device.

Two experiments were performed to study the blocking characteristics of n-GaAlAs/p-GaAs junctions at the doping level to be used in the CG structure. The reverse characteristics of these junctions must be adequate to ensure perfect current confinement to the channel region. P-type substrates were used for the experiment to ensure minimal series resistance effects. Three layers were grown consisting of a p layer of GaAs, an n layer of GaAlAs, and an n layer of GaAs. The dopings and thickness of the GaAlAs layer and the p layer were chosen as being similar to that to be used in actual device structures. 380 x 380 μm mesas were etched through the junction and the n and p sides contacted with AuGe and Ag-Mn, respectively. Devices such as these exhibited sharp reverse breakdown voltages of ~ 11.5 V. The leakage current for these devices was less than 0.1 μA to 0.9 x the breakdown voltage.

In the second experiment, a p layer ($N_a = 10^{18}$ cm^3) was deposited on an n^+ substrate to test the reverse leakage of such junctions and ensure that the

reverse biased junctions would effectively confine the current. 0.050" x 0.05" mesa structures were fabricated by etching techniques and contacted. Individual mesas were probed under light and dark conditions to ensure low enough leakage and photocurrent generation to form good isolation. Leakage currents of less than 10 μA out to the breakdown voltage were observed. For a total laser chip area of 0.02" x 0.02" this would result in a lossy leakage of less than 1 μA. This is more than adequate to provide low leakage current confinement for the stripe region.

The channel guide structure developed on this contract required the presence of a p layer at the substrate interface to confine the current to the center region of the stripe. Two approaches were considered to obtain the current confining p layer: 1) epitaxial growth, 2) diffusion or implantation of an acceptor. The growth of an epitaxial p layer which is subsequently etched and removed in the channel regions was chosen as the current confinement technique. While this process has the disadvantage of requiring two epitaxial growths, it is not considered to be lower yield or under less control than the other processes. In addition, a more perfect resultant crystal is expected with well controlled doping. In addition both diffusion and ion implantation require the use of a silicon nitride overcoat to serve either as a mask or as a cap for annealing. Nitrides are difficult to remove and plasma etching can result in some surface damage.

The channel guide laser structure requires a groove to be etched into the GaAs prior to the growth of the double heterostructure. The requirements of this channel are that it be deep enough to just penetrate the previously grown epitaxial p-layer and yet be narrow enough to provide the necessary current confinement for the device structure. The geometry of the etched groove determines the nature of channel guide structure and must be controllable and reproducible. We have chosen to emphasize the H_2SO_4:H_2O_2:H_2O etching solution as one which is most reliable for the etching of these channels. Figure 2.2.4 shows curves showing the depth of the etched channel as a function of time of etching for a 1:8:10 solution of H_2SO_4:H_2O_2:H_2O at 10°C and 1.5°C. This etch data allows etching of the channel through the epitaxial p-layer, whose thickness will be on the order of 0.5 to 1.0 microns thick. Furthermore, the

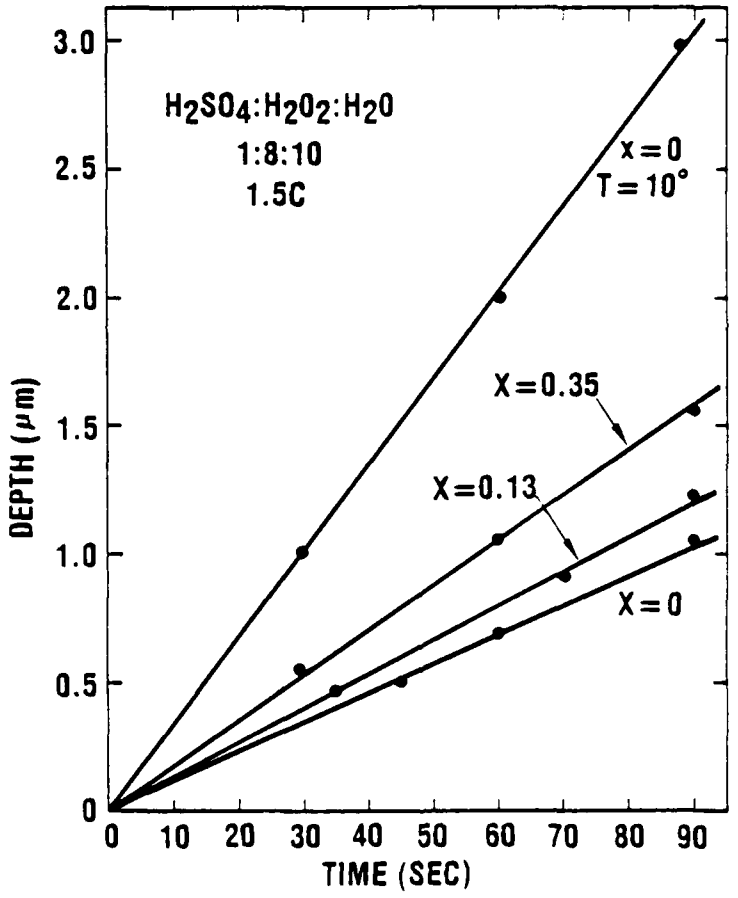

Figure 2.2.4. Sulfuric acid-peroxide water etch for $Ga_{1-x}Al_xAs$.

linearity of the channel depth as a function of etching time will allow the channels to be reproducibly etched to the appropriate thickness. We have used conventional photolithographic techniques in the preparation of grooves for channel guide lasers by using the photoresist as an etch mask. Using these techniques and the 1:8:10 etch solution, grooves with controllable depth and minimal undercutting have been fabricated. These grooves have planar surfaces on both the bottom and both sides of the groove. This results from the exposure of the (111)A planes on the sides of the groove and the (100) plane in the bottom. Figure 2.2.5 shows an SEM microphotograph of etched grooves in a GaAs substrate. Note the planarity of both the side walls and bottom of the etched groove. Part b of the figure shows a cross-sectional photograph revealing the (111)A planes on the side walls and the (100) plane on the bottom of the groove.

Using this etched technique, several channel guide structures have been prepared. One of these is shown in Fig. 2.2.6. A previously grown p-type GaAs layer is covered with photoresist, and the 12 micron wide windows were opened. After etching for about 40 s, a 0.7 micron deep groove is opened through the p-GaAs layer. After removal of the photoresist, the wafer is placed in the reactor, and the remainder of the laser structure is grown. Shown in Fig. 2.2.6 is a structure grown in such a groove. Note that the epitaxial layers follow the contours of the etched groove. This results in the formation of the bent regions of the channel guide structure which in turn will control the mode structure of the active region of the device. Note the planarity of the growth in all regions and the uniformity of the growth. Figure 2.2.7 shows another structure grown on a different wafer in which the groove has been etched considerably deeper, well beyond the zinc doped p-layer on the surface of the substrate. Note again that the layers conform to the groove dimensions and that a beautifully symmetric channel guide structure results.

2.2.4 Inverted Channel Guide Laser

Shown in Fig. 2.2.6 is a channel guide structure with current confinement provided by the etched p region below the active region. These structures have been operated as lasers with average threshold currents (length 300 - 500 um) less 60 mA. Laser operation on a single longitudinal mode proved

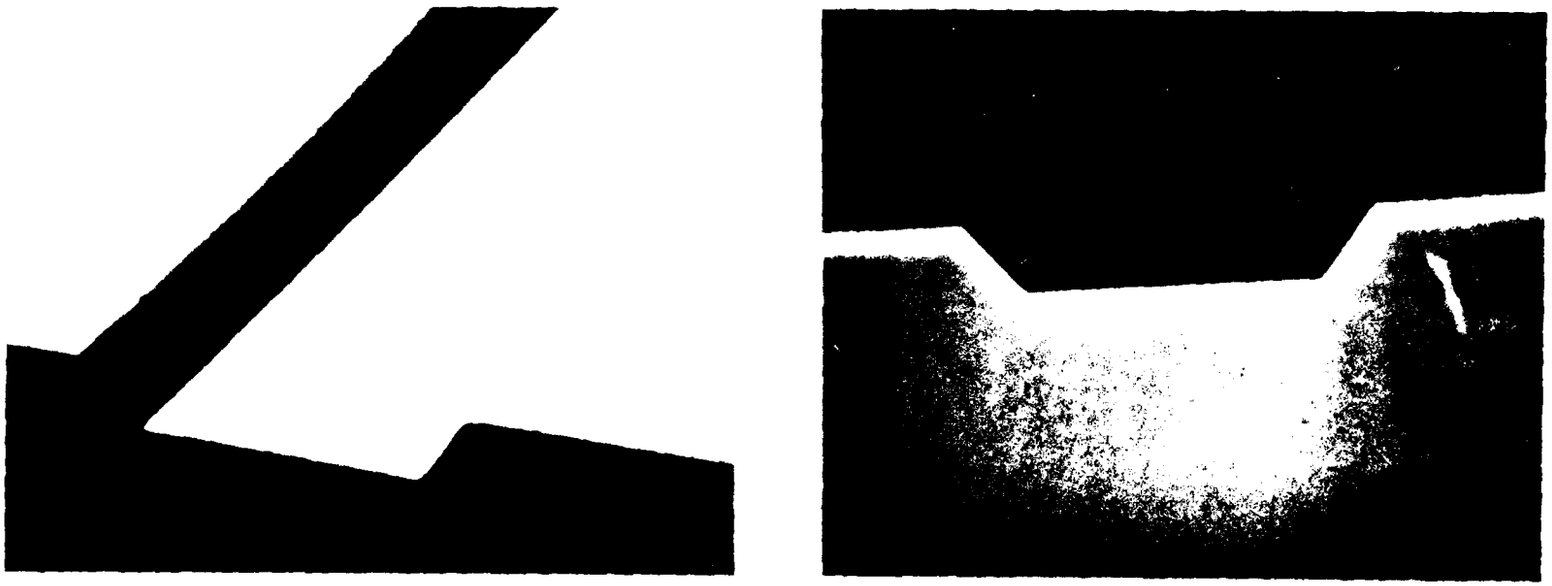

Figure 2.2.5. Etched grooves in GaAs.

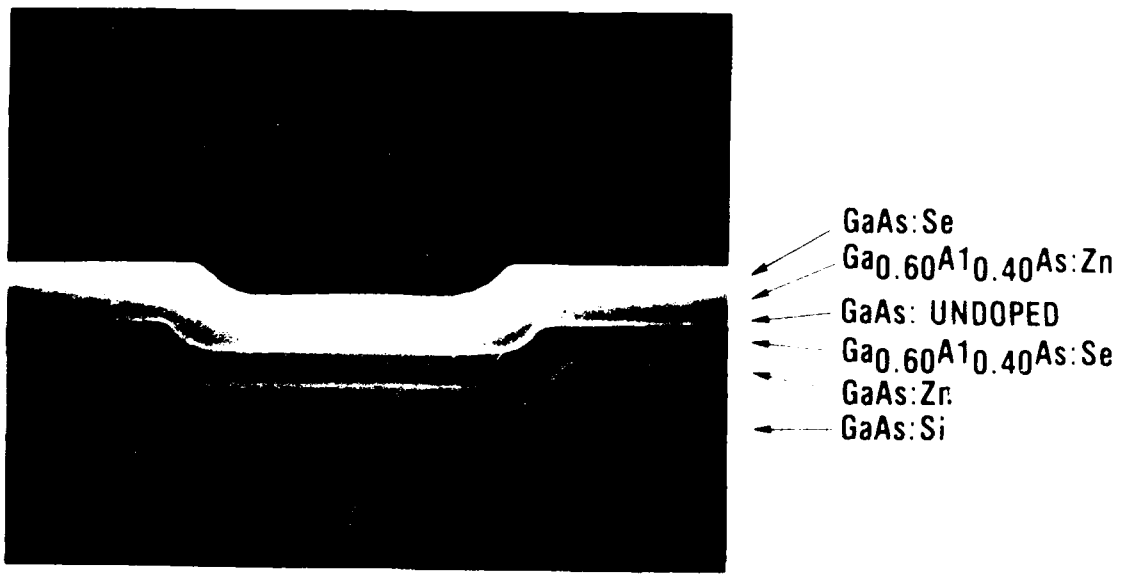

Figure 4.6.6. SEM photograph of a channel guide structure.

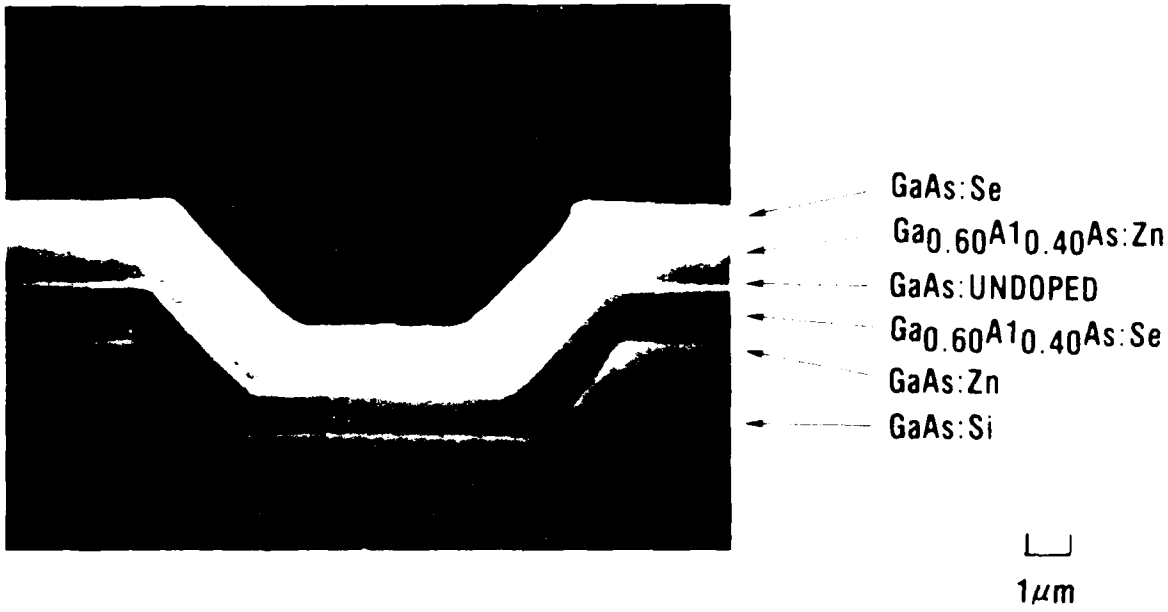

[illegible] SEM photograph of a channel guide structure.

not to be possible, however, since current confinement is not limited to the flat portion of the channel guide. With normal current spreading and the guide corners included in the current stripe, there is too much recombination outside the flat cavity guide region. As a result, the spectra show competition between the mode in the channel and the sidewall mode.

In order to overcome this problem, we have studied an inverted guide structure shown in Fig. 2.2.8. With current confinement from the top surface only, laser operation and reasonable thresholds are possible, but only on multiple longitudinal modes, presumably for the same reasons that the structure of Fig. 2.2.6 operated multiple mode.

A fourth method considered is to use implanted Be to provide confinement on the etched substrate.

2.2.5 Self Aligned Lasers

Work described in the above sections on the curved junction single mode structures has been disappointing. Although low threshold (60 mA) devices have been achieved, single longitudinal mode operation has not been achieved. A fundamental problem with the bent guide structures as described in the previous report has been achieving adequate current confinement without significantly complicating the device processing. No satisfactory technique was discovered.

Owing to these problems, work was directed toward a new structure. This self-aligned structure, shown in Fig. 2.2.9 requires only a single processing step to provide both current confinement and mode control. In addition, the active layer is grown on an unprocessed surface which leads to minimal problems in crystal quality. With this structure we have achieved low threshold current, single longitudinal mode operation with GaAlAs-GaAs.

The GaAlAs-GaAs self-aligned structure double heterostructure is prepared by a two-step, interrupted MO-CVD growth process. In the first growth step a five-layer structure is grown on a (100) oriented Si-doped GaAs substrate. The five layers are (i) n-GaAs buffer layer, 1.5 - 3.0 μm; (ii) n-GaAlAs (x - 0.35), 2.0 μm; (iii) undoped GaAs active layer, 700 - 1000Å; (iv) p-GaAlAs (x = 0.35), 0.2 - 0.6 μm; and (v) n-GaAs, 0.4 - 0.5 μm, or n-GaAs

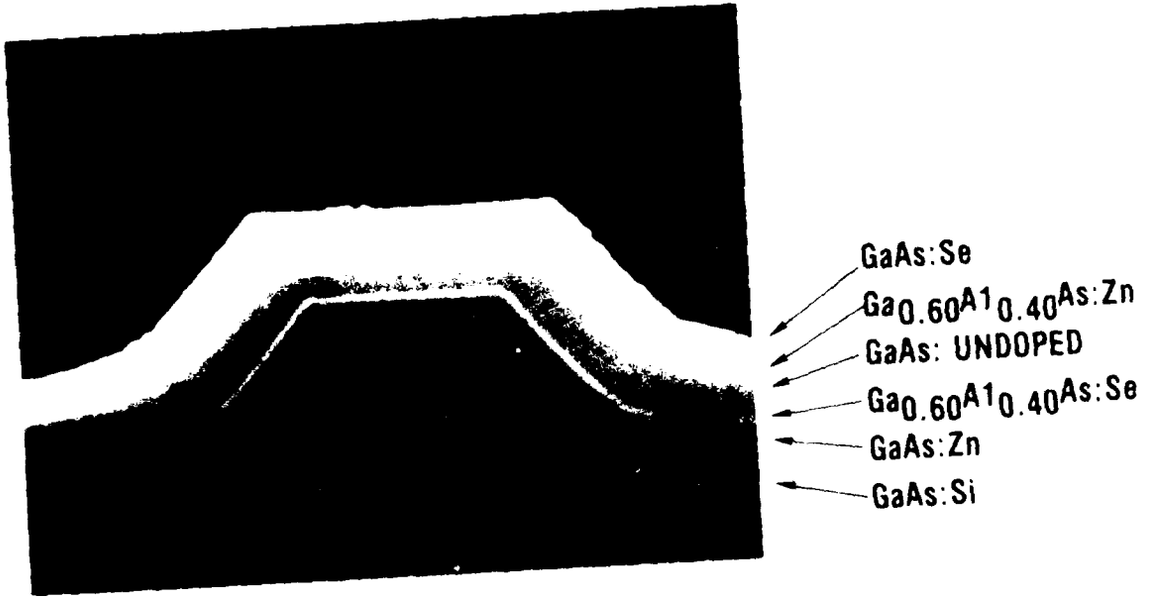

Figure [illegible]. SEM photograph of an inverted channel guide structure.

Figure [illegible] SEM photograph of a self aligned structure.

($x < 0.10$), 0.4 - 0.5 μm. The first two layers are doped with Se ($1 \times 10^{18} cm^{-3}$). The active layer is n type and less than $1 \times 10^{15} cm^{-3}$. The p-GaAlAs layer is doped with Zn ($5 \times 10^{17} cm^{-3}$), and layer (v) is also doped with Se [$(1 - 5) \times 10^{18} cm^{-3}$]. These layers are grown by MO-CVD on a clean GaAs surface which has not been processed in any way, and therefore are of high quality.

After the first growth step, the wafer is removed from the reactor and stripes are opened with conventional photolithographic techniques on the surface along a (110) direction. The widths of the strips used in this work were 4, 6, and 8 μm, not including any undercutting. Typically for a 4 μm nominal mask, undercutting of the etch and resolution limitations of the photolithography result in an actual width at the surface of ~ 5.4 μm. Channels are then etched into the wafer using either a $H_2SO_4:H_2O_2:H_2O$ (1:8:10, 1.5°C) etch or a H_3PO_4-superoxol etch. The channels are etched completely through the n-GaAs layer but only a small distance into the p-GaAlAs layer. A critical feature of this portion of device fabrication is the control and uniformity of layer thickness. The necessary control is easily achieved by MO-CVD.

The wafer is recleaned and replaced in the reactor for the growth of two additional MO-CVD layers. These layers are (i) p-GaAlAs ($x = 0.35$), 1.8 μm; and (ii) p^+-GaAs cap layer for contacts, 0.15 μm. One of the final structures is shown in Fig. 2.2.9. For reference the etched channel width at the top of the n-GaAs confining layer is 5.4 μm. The growth rate of MO-CVD deposition on the (111) planes delineated by the etch is ~ 33% greater than for the (100) plane. Therefore the channel has a tendency to fill, though not completely, during the growth of the p-GaAlAs layer. These different growth rates result in slightly different doping incorporation and lead to the faint, pyramidlike lines in the photograph. Based on the results described below it appears that there is no problem associated with the GaAlAs-GaAs interface which results from the interrupted growth.

Metal contacts of alloyed Au-Ge and Cr-Au are then formed on the wafer. There is no additional current confinement such as an oxide stripe on the surface. Devices are fabricated as usual by cleaving and sawing, with some devices being mounted on headers with In solder for CW testing.

The n-GaAs layer buried in the p-GaAlAs layer serves two purposes. The back-biased p-n junction at the bottom edge of this layer provides current confinement located near the active region. The dimensions and doping level are not trivial for n-type GaAs current confinement layer. The doping and thickness must be designed to fall between the two extremes of tunneling (thin-heavily doped) and punch through (thin-lightly doped). For this reason no additional current confinement is required either above or below the junction. In addition, the presence of a small-bandgap, high-index layer near the active region over most of the cross section provides the necessary effective index change ($\Delta n \sim 0.2$) for passive wave guiding and gain selection and allows the mode control necessary for single-longitudinal-mode operation. For the particular devices discussed below the n-type self-alignment layer is 0.4 μm above the 700A active layer and the etched channel is 4 μm wide.

2.3 Task III - Device Testing

For all of the structures described laser, device testing consisted of pulsed current and CW current measurement of suitably mounted structures. The devices for testing were mounted on TO5 leaders with the solder or held in a pinch-grip test jig designed for quick testing of many laser chips. Near field characteristics of the optical emission were studied with an optical microscope focused on the device facet and a video camera and TV monitor. Far field studies were made with a silicon photodetector and an angular resolved measurement apparatus to yield relative emission intensity in the junction plane as a function of angle. Current-voltage characteristics (CW) were measured directly with a calibrated silicon photodiode and, for pulsed current L-I curves, a Box-car integrator was used in conjunction with the Si detector to provide a gated averaged measurement of the peak light output. Spectral measurements pulsed and CW were made with the emission of the laser routed through a Spex monochromator and into a cooled Sl photomultiplier tube. The output of the tube was amplified and used to drive a chart recorder.

2.3.1 Properties of TJS and Channel Guide Lasers

Little emphasis was placed on the TJS structure measurements. However, the typical laser threshold current obtained from L-I curve zero intercepts was somewhat high (~ 200 mA) and single mode operation was not observed.

Studies on channel guide lasers and inverted channel guide lasers showed characteristics similar to one another. I-V curves showed that in all cases the doping levels in the layers and the quality of the ohmic contacts were sufficient to yield low resistance ideal p-n junction I-V characteristics. L-I curves (Fig. 2.3.1) indicated that laser emission was obtainable at thresholds of less than 50 mA (pulsed) and 60 mA (CW) for devices having 8 μm stripe widths and lengths of 200 μm. In all cases the power output per facet CW exceeded 5 mW at less than 2 X threshold current. Spectral measurements showed, however, that operation was not occurring on a single mode. A typical spectra is shown in Fig. 2.3.2. The two distinct sets of modes in the figure indicate operation in two different filaments. Careful analysis and near field video images confirm that because the current is not confined to the central region of the channel, recombination occurs in the bent sidewall regions as well as in the center. Competition between these sets of modes results in the spectra shown in Fig. 2.3.2. Further confinement of the current proved difficult to obtain and in practice requires many processing steps in order to provide top and bottom confinement, as described in Section 2.2.4.

2.3.2 Properties of Self-aligned Structure Lasers

Self-aligned structure lasers were also tested as described above. These devices had good I-V characteristics similar to those of the channel guide lasers.

Shown in Fig. 2.3.3 is the output power (per facet) versus input current for two self-aligned-structure MO-CVD GaAlAs-GaAs double heterostructures. The curves labeled a) and b) are pulsed room-temperature data for devices 280 and 450 μm long, respectively, with etched widths of 5.4 μm. The current pulses are 100 ns wide and at a 1-kHz repetition rate. For devices with lengths from 280 to 330 μm the average threshold current is less

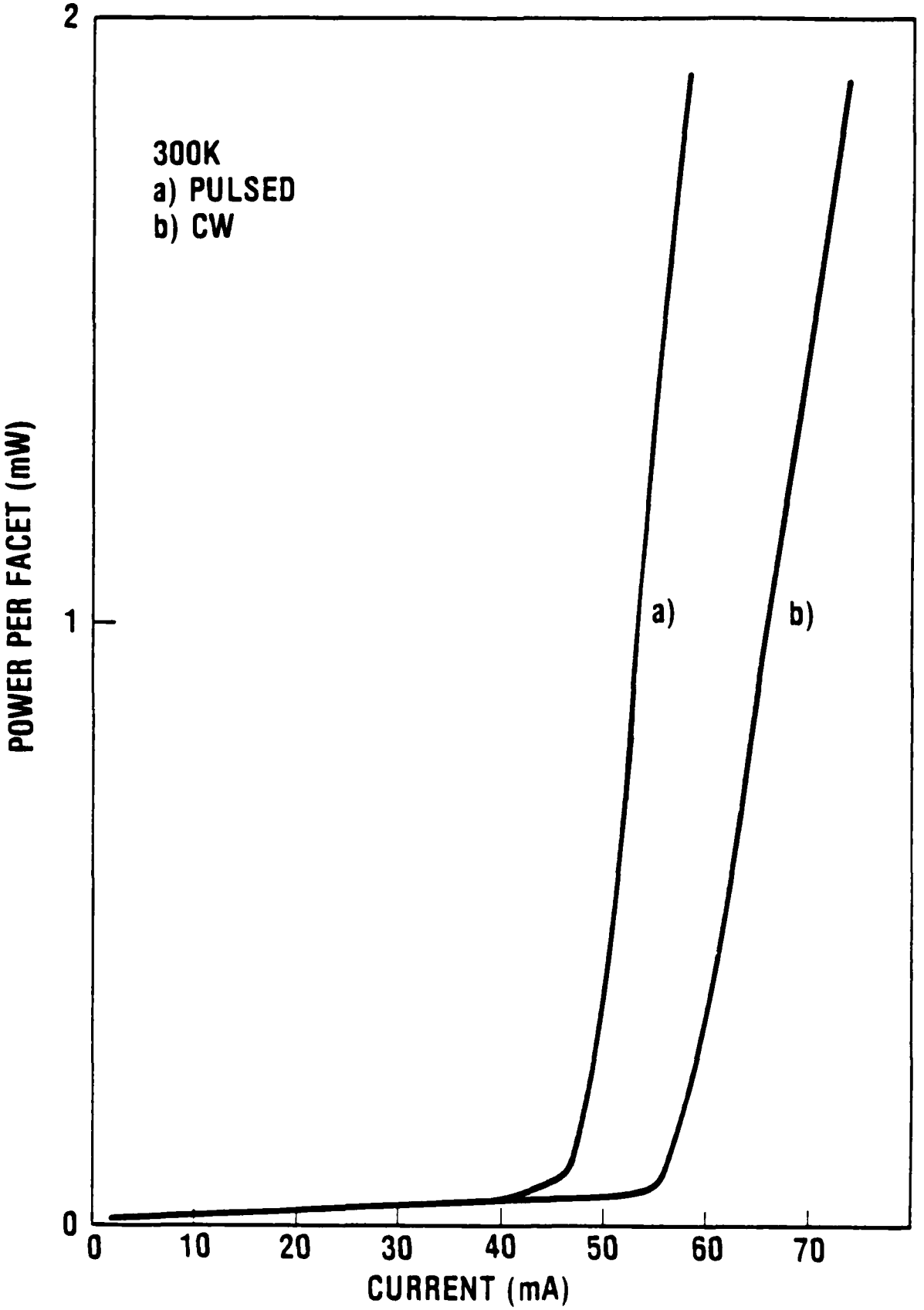

Figure 2.3.1. LI curves for channel guide laser.

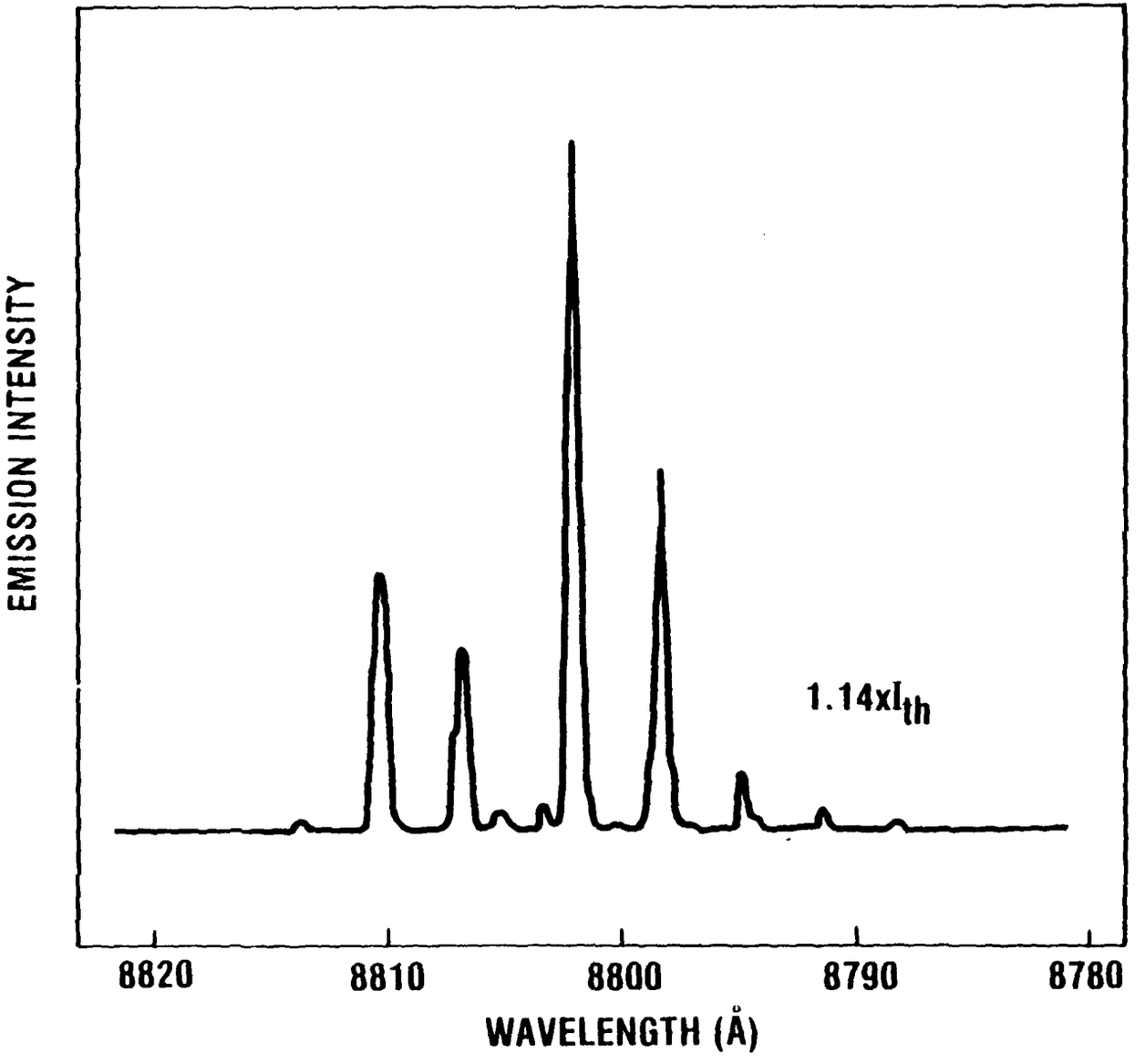

Figure 2.3.2. Laser spectra for channel guide laser.

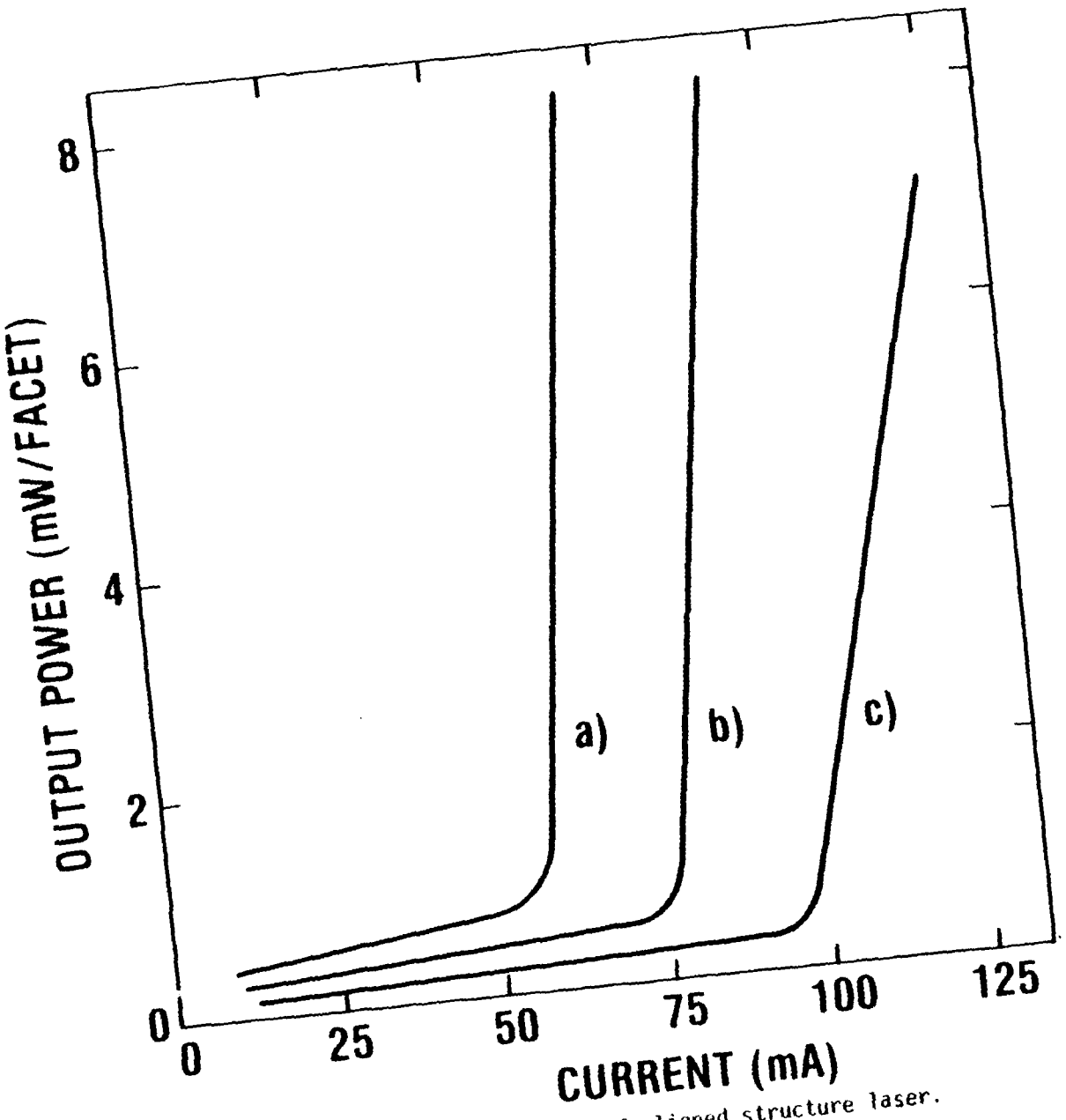

Figure 2.3.3. II curves for self aligned structure laser.

than 60 mA. Curve c) is for CW operation of the same device as b). From these data it appears that the CW device mounting and heat sinking is not yet optimized. For a device 200 μm in length the representative numbers are 51 mA pulsed and 60 mA CW. No kinks have been observed to power levels (CW) greater than 5 mW/facet.

Figure 2.3.4 shows optical emission spectra at various current levels for a self-aligned GaAlAs-GaAs double-heterostructure device 280 μm long (I_{th} = 56 mA). At a current slightly above threshold (59 mA) laser operation on a single longitudinal mode (75 mA) becomes dominant. At still higher current levels (101 mA) the laser emission is still on a single longitudinal mode although the emission has shifted by one mode to longer wavelength. The laser operation for each mode is stable over a current range of more than 10%. The laser emission at 8761Å is stable from less than 90 to greater than 105 mA.

Shown in Fig. 2.3.5 is far field patterns for the self-aligned laser structure up to 1.64 x threshold current. These data show clearly the presence of fundamental mode operation with little feature in the curves outside the main lobe. Full width at half maximum power is ~ 7°.

2.4 Task IV - Device Packaging

The utilization of single mode lasers in practical signal processding applications requires the coupling of the emitted light from the laser into a fiber. This can most easily be accommodated by the utilization of a packaging scheme which includes a fiber pigtail as an integral part of the package. The basic concept for aligning the laser to the fiber pigtail was described in Section 1.2. The use of a silicon submount with preferentially etched grooves to align the fiber was considered to be the technique which would result in a reproducible packaging scheme. The whole silicon submount was to be mounted in an axial TO-5 laser package for subsequent delivery to the Navy. Special provisions in the bonding agents used for both the laser and the fiber as well as the submount were considered so that the total package could be hermetically sealed in the final packaging operation.

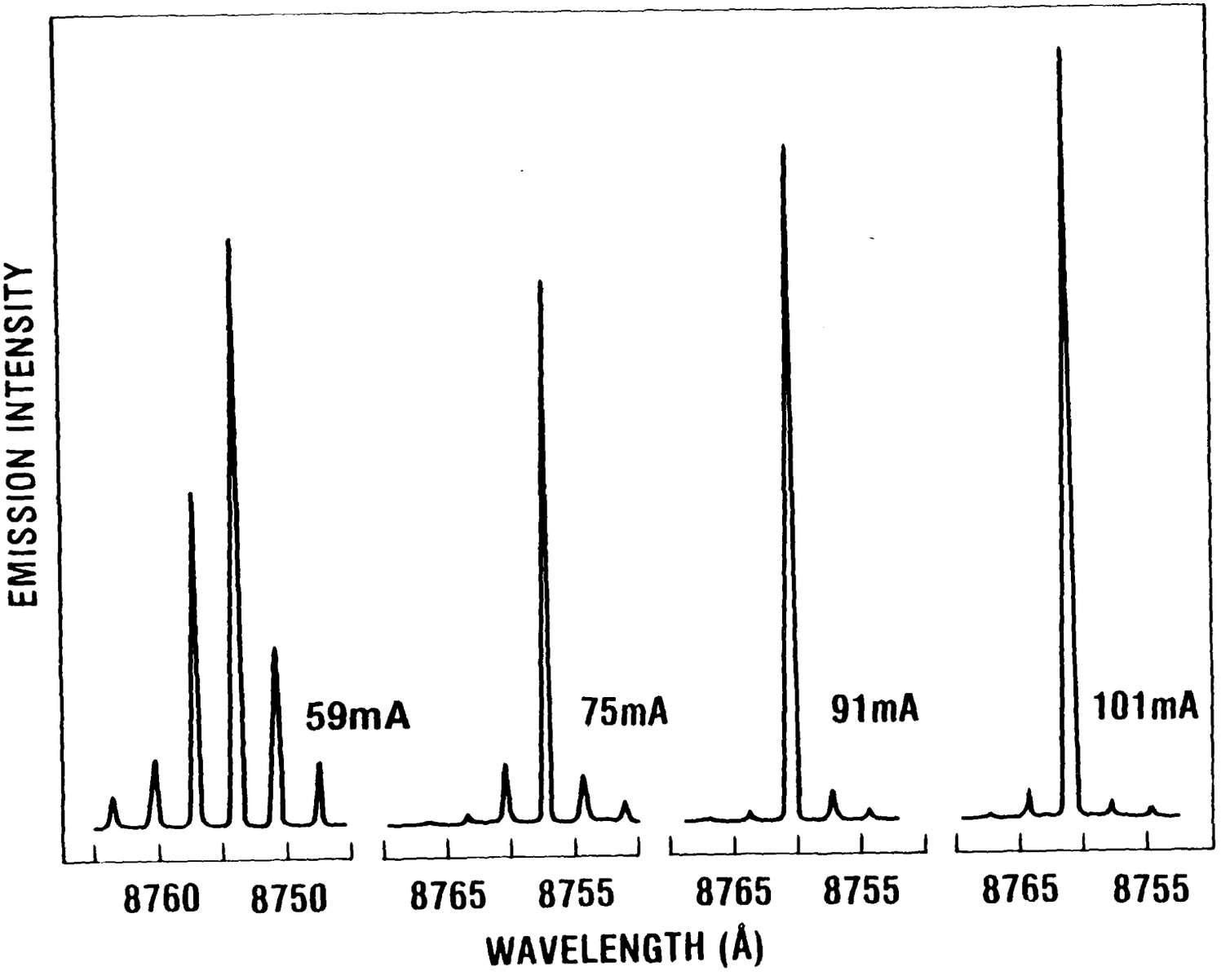

Figure 2.3.4. Laser spectra for self aligned structure laser.

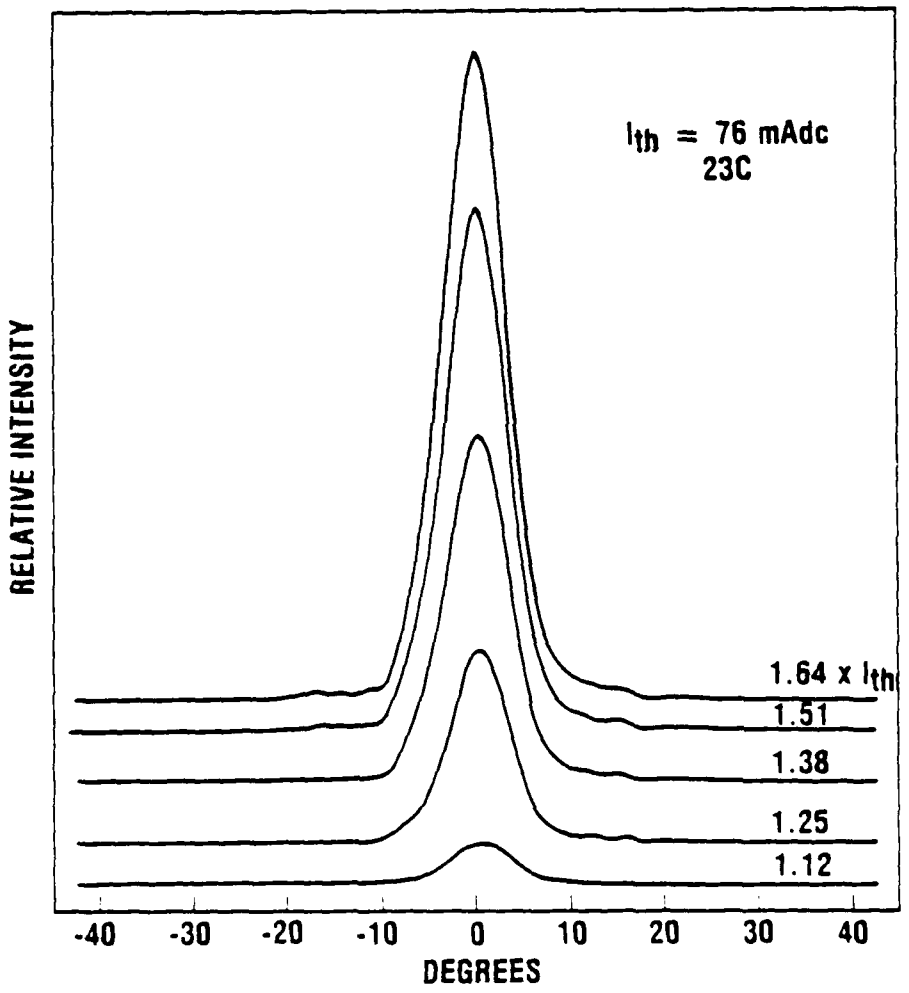

Figure 2.3.5. Far field patterns for self aligned structure laser.

Figure 1.2.1 shows a schematic representation of the packaging scheme to be utilized. The laser is mounted on the silicon submount to which the fiber is bonded using a quick drying epoxy. The submount itself is bonded to a copper stud on an axial TO-5 package. A can is then slid over the entire assembly and the fiber is sealed to the can using either soldering or crimping, and the can is sealed using standard hermetic sealing techniques. This results in a coaxial package which is stud mountable. To achieve this final package, activities in several areas were necessary. Chief among these were chip bonding and fabrication, fiber sealing and package integration.

2.4.1 Submount Fabrication

The use of a silicon submount to align injection lasers to fibers has previously been demonstrated by workers at IBM. The basic concept is to use the capability to preferentially etch silicon to produce V grooves with very precisely controlled dimensions, with sides precisely aligned with thre (111) direction in silicon. By adjusting the width of the V groove, it is possible to precisely align the center of a fiber at virtually any distance each above the surface of the silicon submount. In the application at hand, the laser is to be mounted P-side down on the silicon submount. As a result, the junction will be approximately 2 - 3 μm above the surface of the silicon. With a known diameter fiber, it is impossible to etch the silicon to a precisely determined groove width and align the center of the fiber core wich the junction.

Figure 2.4.1 shows the dependence of the groove width as a function of the height of the fiber above the silicon surface. For the very small displacements of interest in this program, the groove width depends approximately linearly upon the height. Thus, to achieve the appropriate alignment of the laser of the fiber for the use of a 55 μm core fiber, it will be necessary to etch a groove of 150 μm width in the silicon.

In this program, the V grooves were etched using a hot (60°C) alkaline solution consisting of KOH:H_2O:Isopropyl alcohol in the following mixture: 9 grams:30 millilitres:50 millilitres. Representative V grooves etched in silicon using this solution are shown in Fig. 2.4.2. The etching time to achieve

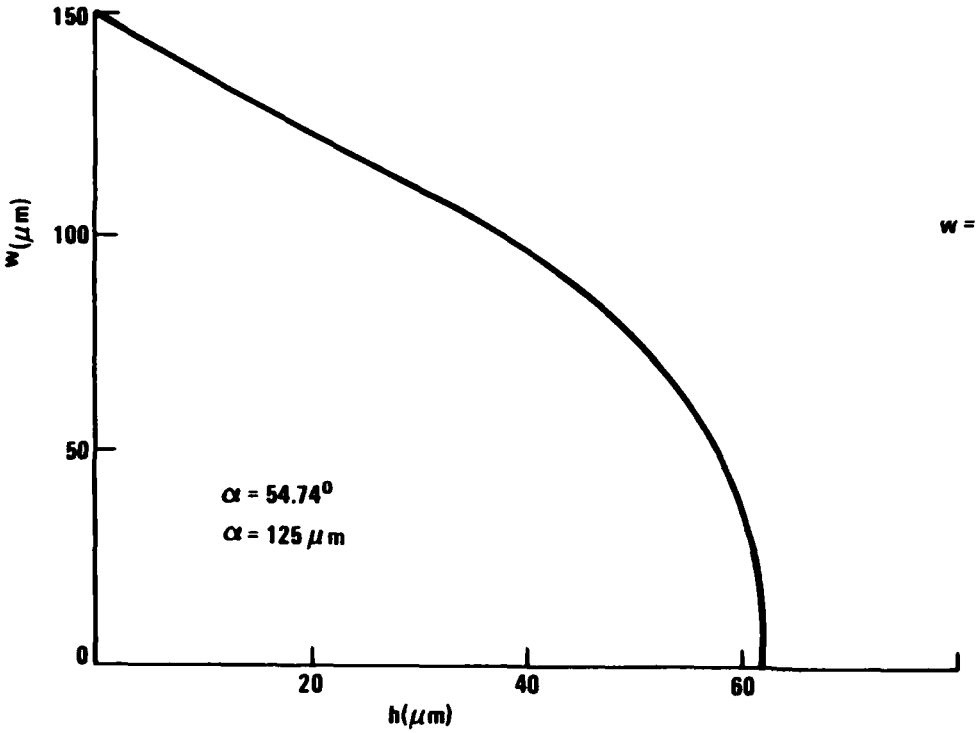

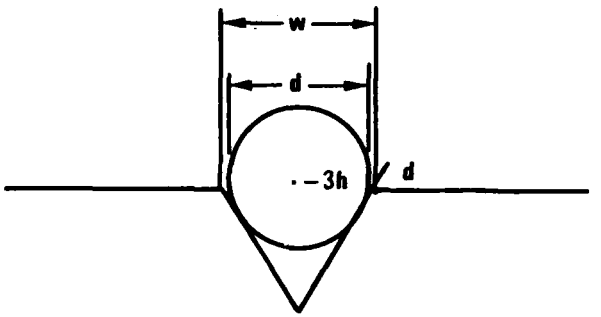

Figure 2.4.1. Groove width as a function of fiber height.

ETCHED V-GROOVES ON (100) SUBSTRATE

Figure 2.4.1. Silicon etched V-grooves.

the V groove shown on the right was approximately 9 hours. The sequence utilized in this program to fabricate the silicon submounted was as follows: Silicon wafers were oxidized to a thickness of about 3000A. A Cr/Au metalization pattern was defined on the silicon to form the bonding pad for the laser. Cr/Au was deposited and subsequently up-plated with indium. After the Cr/Au metalization, the openings in the SiO_2 were made and the grooves were etched to a depth suitable to produce the 150 μm wide grooves. The wafer was then separated and the submounts wre utilized in the fiber alignment experimentation. In some cases, the Cr/Au bonding pads were made directly to the silicon dioxide on the surface of the silicon. In other cases, a special mask was used to allow etching of the silicon dioxide so that the Cr/Au pad could be deposited directly on the silicon submount. The latter case should improve the thermal conductivity of the submount considerably but it did require the subsequent masking of the chrome gold bonding pad during the silicon etching sequence. This proved to be a non-trivial problem and often resulted in substantial yield problems in the fabrication of the submounts. As a result, the results reported in this report are, in many cases, obtained using submounts in which the Cr/Au pad is bonded directly to the silicon dioxide rather than the silicon submount itself.

Figure 2.4.3 shows a photograph of a completed silicon submount. This particular mount contains not only the chrome gold pad and the preferentially etched V groove, but also has indium up-plating on the chrome gold pad to facilitate subsequent laser bonding.

2.4.2 Laser Chip Fabrication and Bonding

To achieve the non-active alignment of the fiber to the semiconductor laser, utilization of V grooves in the silicon submount transfer the alignment problem from that of positioning the fiber properly to that of accurately positioning the semiconduct or laser chip. In a scheme in which active

140

(a) ETCHED GROOVE

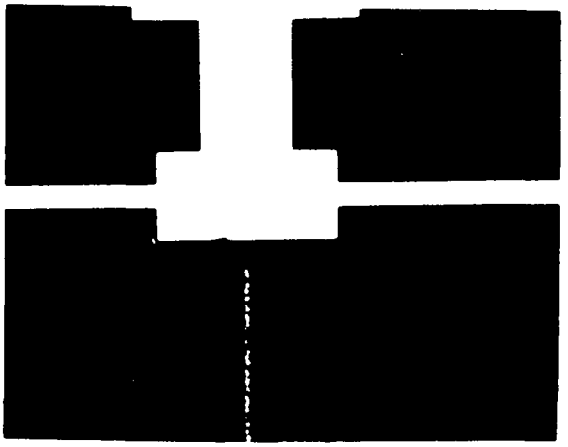

(b) ETCHED GROOVE WITH ELECTRODE

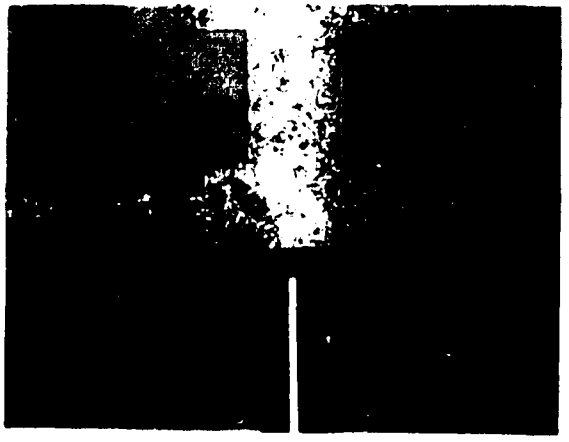

alignment of the fiber is utilized, the chip is bonded to the mount and then the fiber is positioned in the position which maximizes the coupling of light into the fiber. Since the use of the V grooves in the silicon accurately positions the fiber by virtue of the precisely controlled dimensions of the grooves themselves, it becomes necessary to position the laser with respect to the V groove as accurately as the fiber can be positioned. To achieve this, several concepts were explored in the bonding and the fabrication of the GaAs laser. One of the concepts explored was the utilization of a depression in the silicon to accommodate the semiconductor laser in a precisely controlled position with respect to the V groove (see Fig. 2.4.4). In concept, this can easily be achieved utilizing the same etching solution used to etch the V groove. However, it then becomes necessary to utilize a semiconductor chip with reproducible and well controlled dimensions in order that the extra effort involved in etching the alignment depression for the laser would be justified.

To accomplish this required dimensional control on the laser chip, we explored the concept of utilizing preferential etches on the GaAs laser chips to produce V grooves for separation of the GaAs chips. For example, the etching solution, H_2SO_4:H_2O_2:H_2O in a variety of solution strengths, is known to be a preferential etch in GaAs when used to etch features aligned along the (110) direction in GaAs. The solution preferentially defines the (111A) plane depending on the (110) direction can be accomplished by studying the cross section of etches on the small edge portion of the wafer. Utilization of a V groove, after all the chip processing is completed, would facilitate easy and reproducible cleavage of the wafer to a precisely controlled dimension by forming a sharp, pointed stress riser in the wafer.

V grooves were etched in GaAs utilizing a 1:8:1 solution of the sulphuric acid:hydrogen perioxide:water solution described above. This resulted in grooves approximately 75 microns deep and in 15 minutes of etching, using a 15°C solution. These wafers were subsequently back-polished to a thickness of about 0.004". It was then waxed to a flexible metal sheet and the sheet was passed over a sharp edge to initiate cleavage. All of the bars etched into the

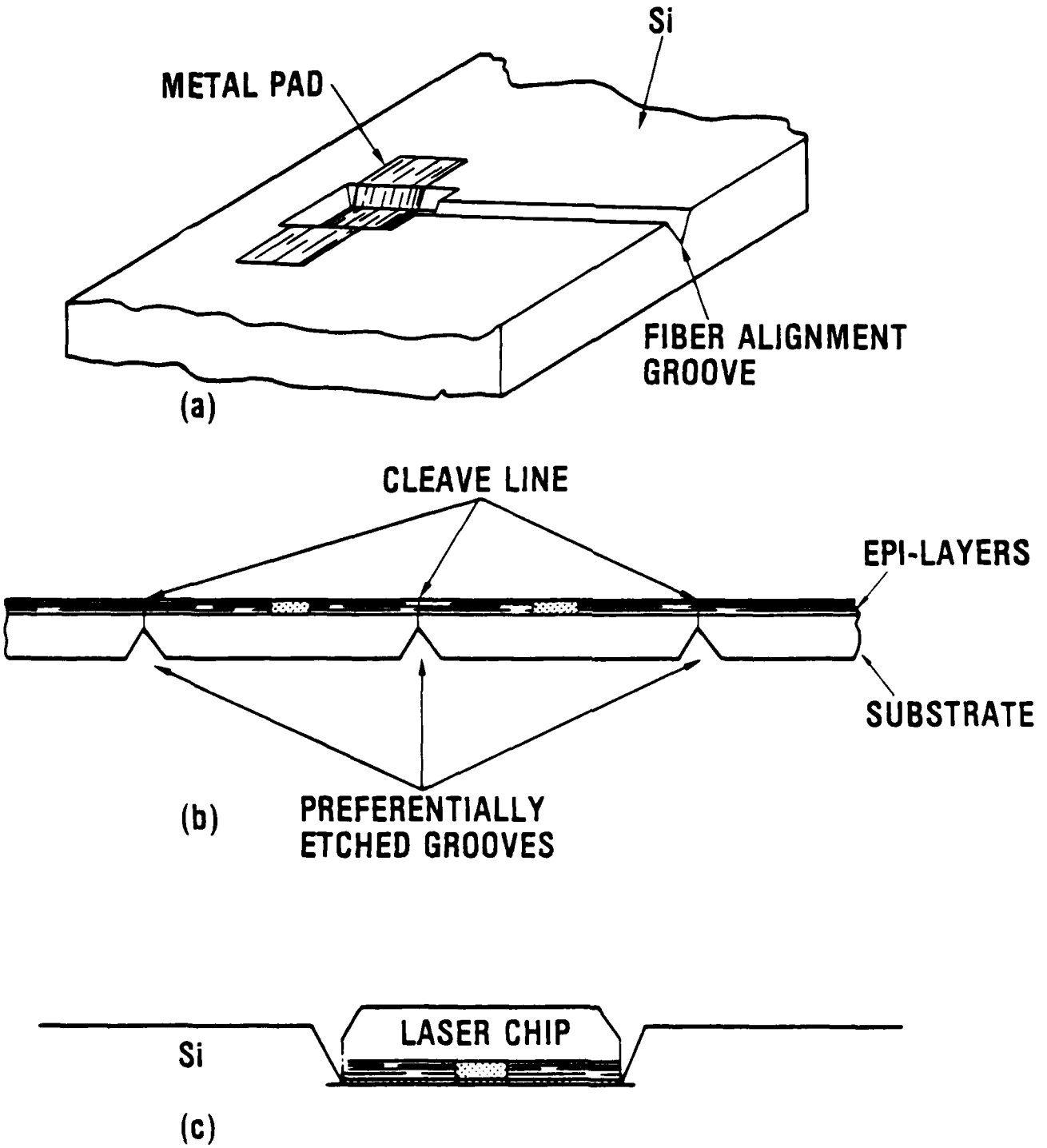

Figure 2.4.4. Etched groove alignment sequence.

wafer cleaved at the point of the V groove along the (110) plane to produce uniform and consistent die shapes.

Figure 2.4.5 shows a cross sectional SEM photograph of one of these cleaved bars. Notice that the cleave that was initiated by the V groove shows no overhanging edges and is a clean, well controlled cleave. The major problem to be overcome in using this technique, however, is the achievement of V grooves with minimal, or at least, well-controlled undercutting of the mask feature on the top surface so that dimensions of the die can be well controlled.

Considerable amount of effort was directed towards finding an appropriate etching solution which would minimize the undercutting of the feature and yet produce a well controlled V-shaped feature. The best selectivity achieved in etching the (110) direction as opposed to the (111) direction, or the planes that form the sides of the groove was only 5:1. Thus, in order to etch a 75 micron V groove, an undercutting of approximately 15 microns was always present. To the extent that this ratio of etching in the two directions is consistent and reproducible, it is possible to accommodate the undercutting by selecting the top surface pattern appropriately. However, it was found that the undercut ratio varied strongly with temperature and solution composition and, as a result, reproducible V-shaped grooves could not be easily achieved. As a result, this approach to alignment of the chip was replaced with another.

During the course of bonding experiments, utilizing both plated indium and indium preforms, it was observed that with sufficient amount of indium on the gold chrome bonding pad, a certain amount of self-alignment of the laser was obtained by the surface tension of the bonding agent as it wet to both the laser and the submount. If sufficient indium were placed on the bonding pad and if the surface of the indium were clean so that it wet to the GaAs chip uniformly, the chip had a tendency to align itself over the Cr/Au pad. To facilitate this self-alignment, the metalization on the semiconductor laser was designed to coincide with the pattern on the Cr/Au bonding pad (see Fig. 2.4.6). Under these conditions, the chip automatically self-aligns to the bonding pad. The chief problem in this bonding operation is the utilization of a sufficient amount of indium to achieve this self-alignment and yet the limitation of the indium so

Figure 2.4.5. V-groove cleaved bar.

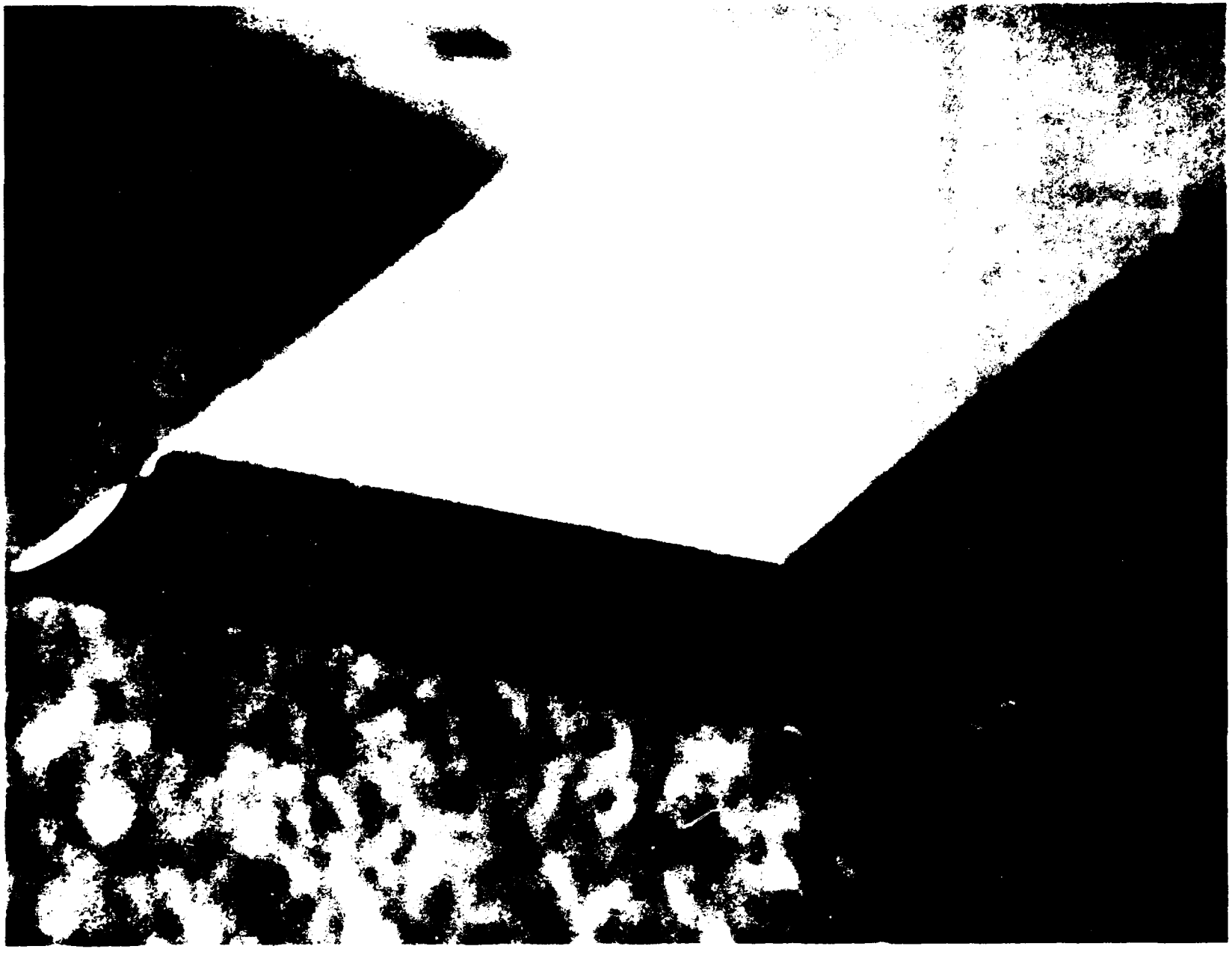

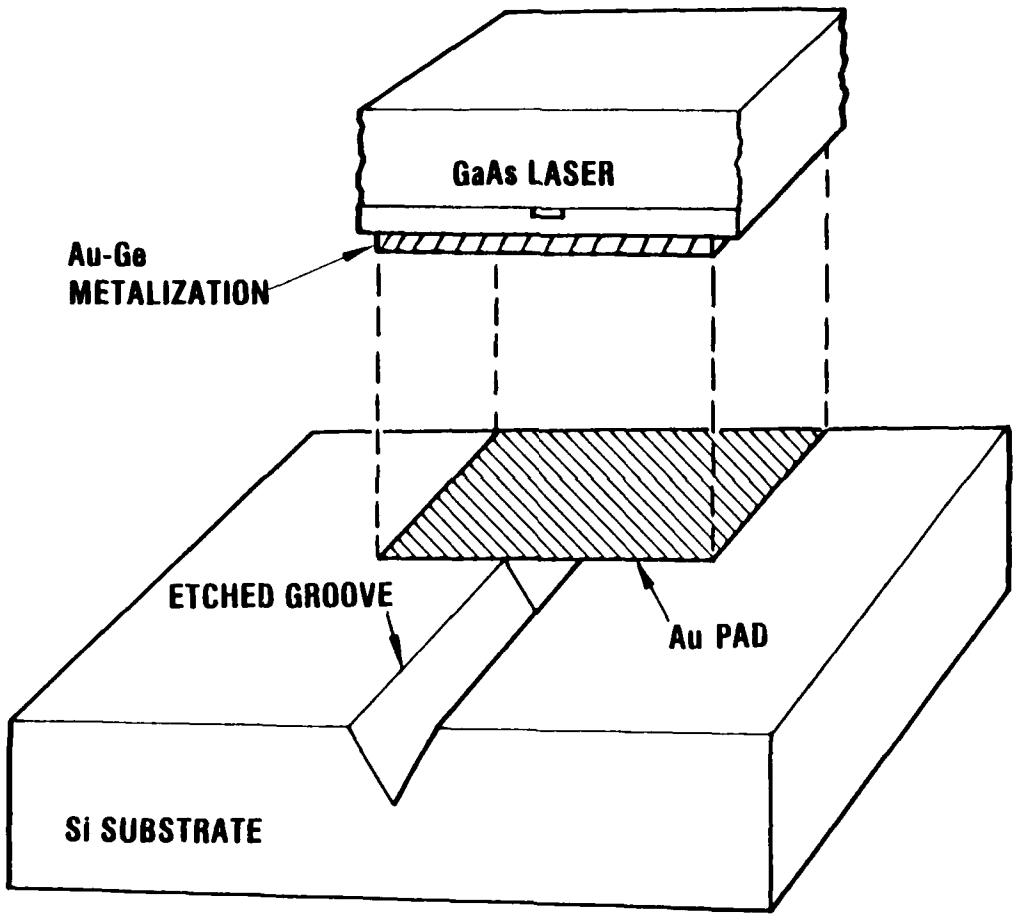

Figure 2.4.6. Schematic of submount alignment.

that the chip is not raised too far above the center of the fiber core. This can, however, be adequately controlled during the plating operation. In all of the deliverable lasers sent to NRL, this alignment scheme was utilized.

2.4.3 Fiber Sealing

The achievement of hermetic seal in the package concept outlined in the introduction to this section requires a hermetic seal between the can and the fiber pigtail. To accomplish this, two approaches were explored. The first was the use of a crimp seal, previously described by workers at Bell Laboratories. In this scheme, a soft, malleable, copper collet is soldered to the can. The fiber is passed through its center. In the final sealing operation, a special instrument designed for this purpose squeezes or crimps the copper collet around the outside of the fiber forming the seal. This approach has the advantage that it is simple to use and does not require metalization of the fiber in order to achieve a good seal. A large number of crimped seals were formed utilizing this technique and excellent fiber to collet seals were achieved. However, it was also observed that during the crimping operation an inevitable movement of the fiber occurred. This typically was in the form of an axial motion. In the package scheme envisioned for this program, such a motion could result in the separation of the fiber from the V groove alignment position and is a definite disadvantage to the sealing technique. In addition, it was discovered that the crimping pressure was very critical to achieving a hermetic seal that did not result in a fragile fiber-to-collet bond. In many cases, when too large a crimping pressure was utilized the transmission of the fiber decreased, the point at which the fiber emerged from the collet became quite brittle and the fiber easily cracked off at the end of the fiber collet sealing position.

The solder sealing technique requires the metalization of the fiber so that an adequate bond between the solder and the fiber can be achieved. Several metalization schemes were explored to determine which could most accurately achieve this bonding function. After some experimentation, it was decided that a Ti/Pt/Au metalization deposited by sputtering was the appropriate answer to this metalization problem, and several fibers were locally metalized for bonding experiments. A special collet was designed in brass to accommodate the solder

sealing operation. In addition to the long, narrow channel for the fiber, there is an opening in the side of the collet to accommodate the bonding operation using solder. After the fiber is passed through the collet, the sealing operation takes place by soldering using localized heating the fiber directly to the collet at this opening. This results in a stress-free seal formed by the solder itself. A large number of these solder seals were formed and leak tested. In all cases, the solder seal met the requirement of Mil Spec 5400E. As a result, it was decided to use this solder sealing approach to seal the fibers in our packages.

2.4.4 Package Integration

The successful achievement of all the elements of the package concept would be meaningless without a package integration concept which allowed each of them to be used individually, and yet result in a total package which could be put together under manufacturing conditions. The package concept described in the introduction of this section lends itself quite well to reproducible manufacturing procedures. Some of the problems which were encountered, however, in the final assembly of packages included the need to utilize a relatively high temperature solder for both the chip bonding and the submount bonding to the header. This results because of the need eventually to seal the TO-5 can to the header in the final sealing operation. This requires the application of localized heat which can, in some cases, be transmitted to the submount and result in melting of soft solder such as indium.

Another problem in the total package integration is the utilization of a bonding agent for the fiber to submount assembly, which does not outgas during subsequent bonding operations, or during long term usage. This is a difficult problem and was not undertaken during the course of this program. Usual laboratory type quick drying epoxys were used to bond the fiber to the submount in all of the packages utilized in this program. A more appropriate technology would probably be to use a solder bonding scheme as was used in the package sealing.

The final assembly of the packages took place in the following sequence: First, the semiconductor laser was bonded to the silicon submount,

aligning the laser appropriately to the silicon V groove. The submount was then bonded to a copper block extension of the TO-5 package. The laser was then wire bonded to the TO-5 package stud and the fiber was inserted in the silicon V groove and attached using a quick drying epoxy. The TO-5 can to which the collet had been soldered is then slid over the fiber and attached to the TO-5 package, using either a welding sequence or a soldering sequence. The pigtail is then sealed to the can using a soldering technique.

3.0 PROGRAM ASSESSMENT

The objective of this section is to critically assess the technical progress achieved in the program and to compare the technical progress to the original program goals.

To accomplish this assessment, this section is divided into three subsections which discuss, respectively, the overall program progress, the progress towards achieving single mode operation with channel guide structures, and the viability of using etched grooves and silicon to align single mode fibers to single mode lasers.

3.1 Overall Program Assessment

The goal of this program was to produce a low threshold, single mode laser which operated continuously at room temperature. More specifically, the device was to have a threshold current of 25 mA and to operate in a single translongitudinal and transverse mode up to power outputs of 4 mW. To be compatible with system requirements for these devices, other characteristics such as beam ellipticity and maximum operating temperature were also specified. In reality, these parameters are relatively easily met by appropriate adjustment of device parameters and will not be specifically compared to the devices fabricated in this program. It is safe to assume that the major program goals are embodied in the title of the device, i.e., low threshold, CW, single mode lasers.

To achieve the program goals, Rockwell developed a new structure that demonstrated all of the above features. The self-aligned GaAlAs/GaAs heterostructure lasers were designed and fabricated which demonstrated the following device parameters: 1) Single longitudinal and transverse mode operation was achieved for currents 10% above threshold up to 50% higher than threshold. 2) Output powers of greater than 10 mW per facet were observed in this current range. 3) CW threshold currents as low as 50 mA were observed for devices 300 microns long x 4 microns stripe width. These same devices also exhibited the single longitudinal and transverse mode behavior. 4) The beam ellipticity was

demonstrated to be 3.5:1. 5) The beam pattern was shown to be totally stable over the entire current range studied. In short, the devices fulfill most, if not all, of the program goals. For example, the 25 mA threshold requirement can easily be met by shortening the device to lengths as short as 100 microns, and by coating one of the facets of the device with a high reflectivity coating. This should easily reduce the threshold current by more than a factor of 2, bringing it well below the 25 mA required for use in this program. The current range over which single mode operation was observed is likely to exceed any range of interest for Navy operation; that is to say the power output of these devices for a drive over threshold of 50% exceeded 10 mW. This output power far exceeds any signal processing requirement that the Navy might envision, even when coupled into a single mode fiber. Similarly, other device parameters can be appropriately modified with slight changes to the device structure.

The superior performance of these devices and their compliance with most of the program goals has resulted in the achievement of most of the program goals. The early stages of this program were devoted to studies of the channel guide laser which will be discussed in greater detail in the next section. As a result, the demonstration of single mode, low threshold operation with the self-aligned structure did not occur until late in the program. The device results demonstrated clearly point out, however, that all of the program goals can easily be met with additional experimental work which was not possible in this program. As will be discussed in the following sections describing future studies, these parameter studies should be completed so that the full capabilities of the self-aligned structure can be demonstrated.

3.2 Channel Guide Lasers

The main thrust of this program, initially, was to investigate the suitability of channel guide structures to meet all of the device parameter goals described in the previous section. This required significant deviation from previous Rockwell work on channel guide lasers. In particular, a scheme to provide positive and total current confinement in the laser structure had to be

derived so that low threshold structures could be achieved. The previous work of Dupuis and Dapkus had demonstrated that lasers with rather high thresholds (approximately 200 mA) could be fabricated using simple oxide isolation techniques. These devices were demonstrated to operate in a single longitudinal and transverse mode. Unfortunately, detailed evaluation of these devices revealed that from wafer to wafer and from device to device on the wafer the laser mode did not occur in a consistent position on the channel guide structure. As a result, the thresholds varied widely from wafer to wafer and from chip to chip and, in fact, the suitability of the device for single mode operation varied widely over the wafer. The techniques employed in this program to provide positive current confinement by the use of reverse bias junctions were not totally successful in the channel guide structure. The reason for this is that, under no circumstances, was it possible to confine the current to the center, straight, portion of the bent channel guide structure. This was an inevitable result of the crystal growth morphology and was not easily remedied by processing tricks subsequent to the crystal growth. In addition, the very non-planar structure which resulted on the surface of the wafer after crystal growth was not conducive to subsequent oxide masking on the top surface to provide a greater degree of current confinement. For these several reasons, it was decided later in the program to abandon the channel guide laser as a suitable structure for low threshold single mode lasers. This decision, which then allowed the effort to focus upon the self-align structure, was necessary to allow the program goals to be achieved. Unfortunately, it could not be anticipated until a great deal of experimental work was done. The results of these experiments are described in the experimental section, Section 2. It should be pointed out that, while the channel guide structure can be made to operate as a single mode structure, it is our present assessment that the structure is not easily configured in a structure that is compatible with low threshold operation.

3.3 Device Packaging

The goal of this portion of the program was to produce a hermetically sealed, pigtailed package containing a single-mode laser. While the ultimate

device would contain a single mode pigtail, our program was to assess the suitability of aligning a graded-index multimode fiber to the single-mode laser using etched V grooves in silicon and to extend this alignment technique, if possible to single mode fibers. In all cases, the alignment was to be a non-active alignment, i.e., one in which the alignment is performed without measuring the coupling of light into the fiber as the fiber is being aligned. It was felt that such a non-active alignment scheme would provide a more manufacturable technique for pigtailing the single-mode lasers.

It should be pointed out that the scheme of using a silicon submount with etched V grooves to align the fiber to the laser transfers the problem of aligning the fiber to the laser to the initial alignment of the chip itself. Several schemes were explored to achieve this alignment in a straightforward fashion. None, however, were totally successful. It appears as though, in order to utilize conventionally accepted bonding techniques that result in strain-free bonding of the single mode laser, it will be necessary to apply a fair amount of "art" to the alignment of the chip. Much of this art has been eliminated by the use of the self-alignment characteristics of the surface tension in the indium solder used to bond the chip to the silicon submount. However, in virtually all cases we have found it necessary to provide small adjustments to the position of the laser to achieve optimal alignment with the silicon V groove. The subsequent bonding of the fiber was performed without the benefit of any minor adjustments to improve the alignment. When the chip was aligned well with the silicon V groove, excellent coupling into the multi-mode fiber was achieved. However, the tolerances for alignment of a multi-mode fiber to the laser being developed in this program are fairly lax, requiring only ± 5 micron accuracy. The use of a 5 micron single-mode fiber, however, would reduce these tolerances to approximately ± 1 micron. It is our opinion that such alignment tolerances cannot be achieved with non-active alignment. As a result, it will be necessary when single-mode fibers are used, to provide some means of manually adjusting the position of the fiber prior to setting the fiber with epoxy in the silicon V groove. This could be achieved in the same fashion that single mode fibers have been aligned to wave guides in lithium niobate by workers at NRL, or

it could be achieved by the use of an external micro-manipulator to align the fiber and hold it in position until the epoxy which is used to bond the fiber to the submount is hardened. Either of these techniques will succeed and the ultimate choice depends upon the facility with which one can align the fiber in a manufacturing environment and the reproducibility of the coupling under these conditions.

4.0 FUTURE STUDIES

A number of studies which extend and complete the studies undertaken in this program are suggested by the successes and failures observed in the course of the experimentation. Perhaps the most important and urgent studies would be further parameter studies of the self aligned laser structure developed late in this program. While most of the program goals were achieved by the use of a "seat of the pants" device design, this device structure can, in no sense, be considered optimized. Detailed analysis of the type carried out for the channel guide structure must be carried out in order to determine the range of device parameters which satisfy the programs goals. Once this range of parameters has been determined, it is then possible to experimentally explore a variation of parameters within this range to determine which device design would result in an optimized structure. For example, the present structure, as designed and fabricated in this program, has a built-in index of refraction along the junction of approximately 10^{-3}. It is possible by appropriate choices of layer thicknesses and composition to greatly increase, or even decrease this index of refraction change. Since the mode guiding which occurs in the structures considerably different than that which occurs in the channel guide structure, it would be interesting to determine how changes in this index difference affected not only the threshold but the current dependence of the mode structure in these devices. At the present time, the devices operate in a single longitudinal mode for currents approximately 10% above threshold. The ideal device would operate as a single mode laser for currents very close to threshold.

Similarly, it might very well be possible to obtain lower threshold currents by the choice of appropriate device parameters. Some variation of these parameters was performed during the course of the experimentation. However, without a detailed analysis to provide a guide to the experimentation, these experiments can only be considered preliminary.

The present structure appears to have excellent current confinement. However, it should be possible to improve this current confinement even more by

the use of a reverse bias jucntion in the substrate itself, using either diffusion or epitaxy. This approach should also be investigated.

Finally, and probably the equal of importance to the initial operating parameters of the device, is the long term stability of these parameters, i.e., the reliability. To date, only limited studies of reliability have been carried out on MO-CVD-grown material. While these initial studies incidate that the devices so fabricated operate with excellent reliability and stability, the devices tested in all cases were grown in a single growth run with no interruption of the growth. It is quite important to discover whether or not the use of an interrupted growth scheme and the positioning of a metallurgical interface ~1000A away from the active region will substantially affect the reliability of these devices. It is our opinion that this is a minor problem. However, such reliability studies should be performed.

5.0 REFERENCES

1. R.D. Dupuis and P.D. Dapkus, Appl. Phys. Lett. 32, 473 (1978).
2. H. Kumabe et al., Appl. Phys. Lett. 33, 38 (1978).
3. K. Aiki et al., IEEE J. Quantum Electron QE-14, 89 (1978).
4. H. Namikazi et al., Appl. Phys. Lett. 45, 2785 (1974).
5. H. Namikazi, IEEE J. Quantum Electron QE-11, 427 (1975).
6. W. Susaki et al., IEEE J. Quantum Electron. QE-13, 587 (1977).
7. Laser Focus, Sept. 1978, p. 44.

DISTRIBUTION LIST

	Quantity
T. G. Giallorenzi Code 5570 Naval Research Laboratory Washington, D. C. 20375	2
H. F. Taylor Code 5570 Naval Research Laboratory Washington, D. C. 20375	1
A. F. Milton Code 5550 Naval Research Laboratory Washington, D. C. 20375	1
D. Lewis Code 221, Office of Naval Research 800 North Quincy Street Arlington, VA 22217	1
Larry Sumney Code 304, Naval Electronics Systems Command National Center #1 - Arlington, VA Washington, D. C. 20361	1
Andrew Glista Naval Air System Command Washington, D. C. 20360	1
Defense Documentation Center Cameron Station Alexandria, VA 22314	12
Naval Research Laboratory Code 2627 Washington, D. C. 20375	2
June M. Nicholson Code 2415 JN Naval Research Laboratory Washington, D. C. 20375	1
Total	22